THE POLAR IONOSPHERE: RESULTS FROM THE ALOUETTE/ISIS TOPSIDE SOUNDERS

by

G.L. Nelms and J.H. Chapman*

Communications Research Center (formerly DRTE)

*Department of Communications

Ottawa, Canada

Abstract

The results obtained from the sweep frequency topside sounder satellites are reviewed. Emphasis is given to high latitude phenomena, and to the possible relation of plasma flow in the magnetosphere to the ionospheric structures observed at high latitudes.

THE POLAR IONOSPHERE: RESULTS FROM THE ALOUETTE/ISIS TOPSIDE SOUNDERS

by

G.L. Nelms and J.H. Chapman*

Communications Research Center (formerly DRTE)

*Department of Communications

Ottawa, Canada

Abstract

The results obtained from the sweep frequency topside sounder satellites are reviewed. Emphasis is given to high latitude phenomena, and to the possible relation of plasma flow in the magnetosphere to the ionospheric structures observed at high latitudes.

I. INTRODUCTION

Satellite-borne sounding of the topside ionosphere began in September 1962 with the launching of the Alouette I satellite. Two years later the fixed frequency topside sounder, Explorer XX was launched, followed in late 1965 by Alouette II and in early 1969 by ISIS-I.

In the second section of this paper there is a brief description of the sounders; in section three there is a description of the various plasma phenomena that have been detected in the sounder data, with indications of their relevance to ionospheric studies. A few very preliminary results from the ISIS-I satellite are also given. The fourth section reviews the present knowledge of mid- and high latitude upper ionosphere obtained by topside sounders and other related experiments.

II. SOUNDER PARAMETERS

A detailed description of the sounders is given by Franklin and Maclean[1]. However, some of the less obvious characteristics that are of importance to the measurements of plasma phenomena are described below.

Alouette I and II contain sweep frequency sounders, covering the frequency range from 0.5 to 11.5 MHz and 0.15 to 14.5 MHz respectively with cycle times of 18 and 30 seconds per ionogram. The ISIS-I satellite contains three sounder experiments; a sweep frequency sounder, covering the range from 0.10 to 20 MHz with a 26 second cycle time, a fixed frequency sounder that can operate continuously for 3.5 seconds, 31 seconds, or 16 minutes on any one of six fixed frequencies, and a "mixed mode" experiment, in which the sounder transmitter operates continuously on a fixed frequency of 0.833 Mc/s

while the sounder receiver sweeps through the normal sweep range from 0.1 to 20 MHz. The three satellites have orbital velocities of about 7 km per second, so the ionogram sampling distance is about 130 km and 200 km for Alouette I and II, and 180 km for ISIS-I. They are in high inclination orbits, 80° for the Alouettes and 86.4° for ISIS-I. All three satellites are still in operation; Alouette I and II now record about 1.3 and 4 hours per day, while ISIS-I operates for about 10 hours per day. ISIS-I contains an onboard tape recorder that is capable of storing just over 1 hour of data. There are currently about 2.5×10^6 Alouette I, Alouette II, and ISIS-I topside sounder records available on magnetic tape; the processing of Alouette II and ISIS-I data into film ionograms is usually accomplished within about 6 months.

As indicated above, each of the satellites is capable of making detailed measurements of the topside ionosphere, along an approximately north - south line, from 80°N to 80°S. These "pole to pole" passes are obtained in about 1 hour of elapsed time, although the local mean time along the sub-satellite track varies by 12 hours; about 5 hours between the inclination latitude and 60° latitude and 1 hour between 60° and the equator.

The sounder pulses are all 100 μsec in duration, and all have rise and decay times of a few nanoseconds. Thus the frequency spectrum of each pulse closely approximates the Fourier spectrum of a square pulse. The first sideband nulls are at ±10 kHz, and the amplitude of the 50th sideband (5 MHz away from the center frequency of the pulse for an idealized rectangular pulse) is only 30 to 40 db less than that of the center frequency.

III. RESONANCES AND CUT-OFFS

It is useful to examine briefly the way in which the plasma resonances and cut-offs observed in the sounder data can be used to measure parameters of interest to ionospheric physics. The frequencies of the resonance spikes yield information on f_N, the plasma frequency and on f_H, the electron gyro frequency at the satellite or various harmonics and combinations of those frequencies. The cut-off frequencies for the various modes of propagation (i.e., the lowest frequency at which the mode can propagate at the satellite) are also determined by f_N and f_H (Fig. 1). Thus, there are a variety of ways[2] of measuring combinations of the electron number density N (from f_N) and the electron gyrofrequency. In practice, the electron gyrofrequency is known accurately, for the region below a few thousand kilometers altitude, from spherical harmonic models of the earth's field, and the various plasma phenomena can be used to improve the spatial resolution of the measurements of electron number density.

Table I lists the cut-offs and resonance spikes[3, 4] that are commonly observed.

TABLE I

Type	Frequency	Plasma relations
<u>Cut-offs</u>		
Z wave	f_{zS}	$f_N^2 = f_{zS}^2 + f_{xS} f_H$ (1)
X-wave	f_{xS}	$f_N^2 = f_{xS}^2 - f_{xS} f_H$ (2)
O-wave	f_N	
Z infinity	f_{zI}	$f_N^2 = \frac{f_{zI}^2 (f_{zI}^2 - f_H^2)}{f_{zI}^2 - f_H^2 \sin^2\phi}$ (3)
<u>Resonance Spikes</u>		
plasma frequency	f_N	
electron gyro frequency	f_H, $2f_H$, --- nf_H	
upper hybrid frequency	f_T, $2f_T$	$f_N^2 = f_T^2 - f_H^2$ (4)

ϕ is the angle between the wave normal and the direction of the earth's magnetic field.

Several less common resonances are observed that are also determined by various combinations of f_N and f_H, as shown in Fig. 2 and Table II.

TABLE II

Type	Frequency	Plasma relations
Plasma frequency harmonic[5]	$2f_N$	
Bernstein wave resonances[6]	$f_{Qn}(n = 2,3,4)$	$f_{Qn} = nf_H + \frac{.464}{n^2}\frac{f_N^2}{f_H}$ (5)
Floating spike[7]	f_{FL}	$f_{FL} = \frac{f_T}{2} = f_N - f_H$ (6)
Mixing[8]	f_{mix}	$\begin{cases} n\, f_{mix} = \text{a resonance frequency} \\ (n+1)\, f_{mix} = \text{a different resonance frequency} \end{cases}$
Diffuse[9]	f_D	$f_D \simeq \frac{3}{2} f_H, \simeq \frac{f_N}{2} \simeq \frac{f_T}{2} \simeq \frac{fxS}{2}$

As well, there are a number of resonance phenomena that reveal additional information about the plasma (Figs. 3-6) as shown in Table III.

TABLE III

Type	Frequency	Plasma relations
Remote resonance[10,11,12,13]	f_c	$f_N = \sqrt{2}\, f_c$ at level where $f_c = 2f_H$
Ionospheric resonance echoes[14,15]	f_N	
Proton gyroresonance[16,17,18]	f_{PR}	
Resonance beats[19]	Δf	$f_N^2 = (2f_H + \Delta f)\Delta f$ for conditions of N<140 el/cm^3 (7)

The remote resonance provides a useful way of determining accurately and simply, without performing an N(h) reduction, the electron density at a height other than the satellite. The remote resonance frequency is equal to the X-wave reflection frequency, fx, at the real height in the ionosphere where $fx = 2f_H$ [$f_N = \sqrt{2}\ f_H$, using equation (2)]. This frequency can be read directly from the ionograms and is called, for convenience f_c (Fig. 3). Since the height variation of $2f_H$ is known from magnetic field models, the height at which $2f_H = fc$ is readily determined.

The direct information provided by the proton gyroresonance is not of particular interest in the region below 3000 km, since the proton gyrofrequency is known as accurately as the magnetic field. This resonance does, however, indicate by its presence that significant amounts of H^+ are present.

The Resonance beats are possibly the most important of the resonance phenomena that have so far been observed, because they provide an entirely new experimental technique for making measurements in a tenuous plasma. For the Alouette II orbit, f_H (and hence fxS and f_T) is always above 0.22 MHz but at high latitudes and altitudes f_N is often less than 0.15 MHz (N less than 280 electron/cc), the low frequency limit for the Alouette II sounder. From equations (2) and (4), as f_N approaches zero, fxS approaches f_T which approach f_H. Since the frequency resolution under these circumstances is usually no better than the bandwidth of the transmitter pulse ($\approx$15 kHz), the frequencies at which fxS, f_T, and f_H occur are too closely spaced for separate identification. However, for electron densities less than about 140 electron cm^{-3}, $f_T - f_H$ is less than 10 kHz, and the transmitter pulse will energize both resonances simultaneously. The difference frequency, Δf, may then be observed as a beat

or modulation pattern (Fig. 6) on the closely spaced f_T and f_H resonances[19]. Since f_H can be determined from the $2f_H$ spike ($\sim$ 2% accuracy) or from a spherical harmonic field analysis, f_N can be calculated from a knowledge of Δf, according to equation (7).

$$N = 18.6\ mf_H \qquad (8)$$

where m = number of cycles of modulation per 200 km range, N = electron number density in electrons/cm^3 and all frequencies are in MHz.

Electron densities as low as 8 and as high as 140 electrons/cm^3 have been measured from the Alouette II ionograms using this method. The upper limit is set by the telemetry bandwidth and the electron gyrofrequency, and should be about 145 electrons/cm^3 for the Alouette II orbit[20]; the lower limit is set by f_H and the duration of the f_T and f_H resonance spikes, and should be of the order of 1 electron/cm^3 for the Alouette II orbit. However, for m less than 1 cycle per 1000 km (N $\approx$ 5 electrons/cm^3) identification of the modulation pattern on Alouette II ionograms would probably become difficult.

Because this method of measurement depends upon the response of a volume of the plasma around the spacecraft, rather than on the collection electrons, it is the only known method at the present time of measuring accurately low electron number densities (most probes encounter difficulties below a few hundred electrons/cm^3) and the method has been used to provide an in-flight calibration at low densities of the cylindrical electrostatic probe on Alouette II[21] and of the ion mass spectrometer on the sister satellite, Explorer XXXI[22]. It is expected that it will be used extensively to provide similar calibrations of other probe experiments in the future.

One of the major discoveries from the Alouette II satellite was obtained by this method of measurement. It is that electron densities over an extended area of the polar region often fall to less than 30 electrons/cm^3 at altitudes as low as 2000 km, and are occasionally as low as 8 to 15 electrons/cm^3 below 3000 km[19]. Some of the results of studies of the low density regions, obtained by this method of measurement, are summarized in section IV of this paper.

III.2 The Mixed Mode Experiment on ISIS-I:

Figures 6a and 6b are examples of records taken in the mixed mode of sounding from ISIS-I. In this mode, the frequency of the sounder pulse transmitter remains fixed at 0.833 MHz (f_{Tx} on Figs. 6a and 6b) throughout the normal frequency sweep of the receiver. The results from this experiment were somewhat surprising; Fig. 6a shows that all of the common resonance spikes are stimulated by the transmitter, regardless of their proximity to the transmitter frequency. In this case f_{Tx} is close to the second harmonic of f_H; other records in this pass show that similar results are obtained even when f_{Tx} is not near any of the plasma resonances or cut-offs, except that the gyrofrequency harmonic spikes are enhanced when one of the f_H harmonics corresponds to the transmitter frequency.

Figure 6b was recorded in conditions of spread F when strong ducting is likely; even the Z-, O-, and X-wave reflection traces were observed while the sounder was in the mixed mode. At 3.0 MHz the sounder was switched from the mixed to the normal mode of operation, and the usual strong spread F traces are seen for the remainder of the record.

The stimulation of resonances and reflection traces at frequencies well removed from the transmitter frequency is thought[23] to be due to sideband energy in the Fourier spectrum of the rectangular transmitter pulse. As was pointed out in section II, the amplitude of the 50th sideband of an idealized rectangular pulse would only be 30 to 40 db less than that at the centre frequency.

IV. RESULTS

The ionized region above the main peak of the F layer can be studied from many points of view, and because of the complexity of the region, no single simple theory is likely to be adequate for an understanding of the region. However, because of the increasing influence of field and plasma flow effects with increasing height, it is useful to review the knowledge of the region in terms of the major types of structures that are observed, and to try to relate these observations to the main constricting forces present in the magnetosphere.

Although by no means a surprise, one of the striking results from the topside sounders is the extent of the control that the earth's magnetic field exerts over the distribution and movement of ionization. Since details of the observations of most of the irregular structures observed in the topside ionosphere have been in the literature for some time, only the principal results from the studies will be reviewed in the following.

IV.1. Occurrence of Irregularities in the Topside Ionosphere

Irregularities are observed in two distinct areas of the topside ionosphere, a polar zone and an equatorial zone, and both occurrence and propagation characteristics are somewhat different in the two regions (Figs. 7 and 8).

Although this paper is mainly concerned with the polar ionosphere, scattering in the equatorial ionosphere is of interest because of the insight it gives on processes in the polar regions.

Weak spread F is usually observed on ionograms recorded at geomagnetic latitudes greater than about 50° to 60° during the day time, and about 45° during the night. During the day the transition from ionograms exhibiting spread F to no spread F is often abrupt and occurs over a few degrees of latitude.

During magnetically quiet conditions, the region of strong spread echoes at 1000 km is confined to geomagnetic latitudes north of 75°N at about noon local time. The region moves from north to south before midnight and south to north after midnight. It reaches a minimum latitude of about 75°N around midnight. The latitudinal variations of the strong spread echoes are similar to those of sporadic E, visual aurora, radio blackouts and horizontal deviations of the earth's magnetic field[26].

In the polar zone, it is difficult to compare bottomside and topside data because auroral absorption and polar blackout often obscure spread-F observations made from the ground[27]. At other latitudes the major features of the two occurrence patterns agree[28]. The major differences are secondary maxima above the F-region peak during the day in the equatorial region and generally higher occurrence above the F-region peak than below.

IV.2. Spread F and Ducting in the Equatorial Topside Ionosphere

Spread F is particularly interesting in the equatorial region, because of the insight it gives us into the mechanism of diffusion of irregularities of ionization along the magnetic field lines, and the striking propagation effects which are observed.

Lockwood and Petrie[28] identified echoes scattered from irregularities aligned along the equatorial magnetic field, forming a shell of ionization extending many km in the E-W direction. Alouette I at 1000 km altitude (Fig. 8) usually passed over this region, but Alouette II and ISIS-I, having perigees several hundred km lower, occasionally pass through this shell of irregular ionization. Fig. 9 shows such an example from ISIS-I.

In Fig. 9A the ISIS-I satellite was just outside of the sheet, resulting in reflections from the sheet which exhibit a sharp upper boundary that is located just a few km from zero range over a frequency range of several MHz. On the ionogram of Fig. 9B, recorded 60 seconds and 400 km later, the satellite was inside the sheet. Only a scatter signal is observed from propagation in the vertical direction (e.g., 5 to 9 MHz at about 500 km range); most of the energy is guided along the field, within the sheet, to the reflection level in the near (S) and in the far (L) hemisphere. The remarkable ε shaped trace is due[23] to the one "hop" of propagation to the far hemisphere (L) for the upper part of the ε, two hops to the near and one to the far hemisphere (2S + L) for the bottom part of the ε. The center bar of the ε is due to an S + L hop, and is horizontal because the S and L traces happen to be nearly mirror images. That is, as the frequency increases, the increase in path length is balanced by a decrease in retardation. This record is by no means a unique example of such a coincidence; it has been observed on several other ionograms. No clear examples have yet been obtained of the satellite emerging below the sheet, so it is likely that the sheet is much thicker than the 50 km originally postulated by Petrie and Lockwood.

Propagation along field-aligned ionization irregularities[29] (ducting), between the satellite and reflection points in the near and far hemispheres, is a common feature of mid and low latitude topside sounder ionograms. On occasion 10 consecutive hops between hemispheres have been recorded. The distance travelled by the waves on this occasion was equivalent to once around the earth.

Several studies have been made of the occurrence of field-aligned propagation, and the size of the structures that guide the waves[29-33]. Several of these authors have used ray-tracing techniques to demonstrate the mechanism of radio wave propagation back and forth along irregularities of ionization aligned along the magnetic field. One condition for a ray to become trapped by a field-aligned sheet of ionization is that the ray must be very nearly tangent to the sheet. As the frequency is increased, this condition is satisfied at lower heights in the ionosphere.

Scattering and ducting by irregularities are intimately associated in the equatorial region. Pitteway and Cohen[34] suggested a combination of vertical and ducted propagation as an explanation of "frequency spreading" observed on equatorial bottomside sounder ionograms, and Muldrew[29] showed that this "combination mode" was a common form of spread F on topside sounder equatorial ionograms. Calvert and Cohen[35] proposed that "range spreading" on equatorial bottomside sounder ionograms was due to aspect sensitive backscatter from ionization irregularities elongated along the field. Dyson[32] showed a close correlation between scattering and ducting, with ducting more common at low latitudes and scattering more common at high latitudes. Loftus et al[30] found that scattering occurred only in the presence of ducting in the low and mid latitude regions.

Figure 9B is particularly interesting since it shows about four extra-ordinary wave traces which are evidence of propagation along ducts in which the average ionization was significantly different; the main trace is the strongest signal occurring at the lowest frequencies, therefore indicating in this case that the ducts contained an excess of ionization over the ambient.

IV.3. Spread F and Scattering in the Polar Topside Ionosphere

Somewhat analogous phenomena have been observed in the Arctic ionosphere. However, since the lines of the magnetic field stretch much farther into space than in the equatorial regions, and at high latitudes are swept out into the tail of the magnetosphere, conjugate ducting is not observed. Petrie[36] has observed spread echoes from consecutive Alouette I ionograms which first decrease to zero range, and then extend again, indicating that the satellite has passed through a near vertical sheet of irregular ionization at 1000 km height.

Figure 7 shows an example of reflections from such a sheet. In this case the sheet was magnetic field-aligned and about 100 - 200 km thick transverse to the field. The deviations in electron density are sufficiently large to scatter signals 2 MHz or more above fxS. In the ionogram of Fig. 7, backscattered signals of this type appear between 200 - 300 km apparent range and about 2.5 to 4.5 MHz on the frequency scale.

Calvert and Schmid[24] proposed backscatter from long, thin field aligned irregularities as the dominant mechanisms for producing spread F. Calvert and Warnock[27] suggest that the disappearance of directed echoes at high latitudes may be due to their being masked by scatter echoes. However, there is an alternate explanation for spread F that does not require either field-aligned irregularities or ducting[37,38].

IV.4. Precipitation Boundaries at High Latitudes

The ambient density distributions are also governed in a major way by the presence of the field, not only to the extent of forcing diffusive equilibrium, if and when it exists, to occur along the field rather than in a vertical direction, but also because the field lines that are closed to the opposite hemisphere provide a major restriction to the free flow and distribution of ionization that is not present where the field lines are open into the large volume of the magnetospheric tail[39,40]. The boundary between these two regions, those of open and of closed magnetic field lines, is the boundary of major significance in the high ionosphere, and is probably of greater importance in the low ionosphere than has thus far been recognized.

IV.4.1. Particles of Energy > 35 keV

McDiarmid and Burrows[41] defined several boundaries found in the energetic particle data from the Alouette II satellite. They found that for Kp < 2⁻ between December 1965 and July 1966, the "background" boundary for 35 keV particles, which they regarded as the limit of the closed field lines, varied between about 70° geomagnetic at 2100 LMT at 77° at 0800 hours, whereas the "smooth" boundary, which they interpreted as the limit of stably-trapped electrons, varied between about 67° at midnight and 70° at 1100 LMT. The low latitude boundary of the region of maximum frequency range for Spread F echoes, observed by Petrie[26] from Alouette I ionograms, is in good agreement with the "background" boundary of 35 keV particles.

Hartz and Brice[42] combined a wide variety of upper atmosphere phenomena that they considered to be linked in some way to the influx of auroral particles, into an idealized representation of two main zones of

auroral particle precipitation in the northern hemisphere (Fig. 10). They considered the outer zone to be associated with a particle influx that was steady and widespread, and which they described as a "drizzle", and the inner zone to be associated with intense and spatially limited events which they called, after O'Brien[43] "splash". The splash boundary should occur very close to the boundary between the open and closed field lines. It should be noted that the McDiarmid and Burrows[41] and Petrie[26] data are included in the data used by Hartz and Brice. In Fig. 10 two curves are added to the original Hartz and Brice diagrams; the most recent determination by McDiarmid and Wilson[44] from the Alouette II particle data, of the boundary of the closed field region, and a line estimate of the Hartz and Brice splash boundary. These curves will be used for comparison later in the paper (Fig. 11).

IV.4.2. Low Energy Electrons (E < 1 keV)

The precipitation of low energy electrons (E < 1 keV) is of particular importance in the topside ionosphere because such particles have their maximum ionization effects above about 150 km (above about 250 km for 500 eV electrons[45]). Very few measurements exist of near thermal particle fluxes. However, a few general comments can be made on their behaviour from the measurements that do exist[101,102] and by extrapolation from measurements of more energetic particles[46].

(a) In the tail of the magnetosphere low energy electrons are found near the neutral sheet and are distributed across the tail from dawn to dusk, corresponding to an extension of the sheet. They are much

more numerous on the dawn than on the dusk side, with maximum population at 0400 and 1900 magnetic local time.

(b) The spectrum of low energy electrons softens with increasing geocentric distance, and the less energetic the particle, the higher the geomagnetic latitude at which it is precipitated.

(c) The high latitude boundary of trapped electrons of energy 280 eV < E < 2.7 keV is at 74° to 76° geomagnetic on the evening side and 73° to 74° at midnight. Outside this boundary there are occasional intermittent "islands" of such electrons.

The boundary given in (c) is well outside the region of stably-trapped 35 keV electrons given by McDiarmid and Wilson[44], but is approximately coincident with their limit of the closed field lines (see Fig. 10).

Maehlum[47] observed electrons of 50 eV to 1 keV in the polar regions, between 71° and 84° geomagnetic latitude. He found that these electrons showed a strong GMT control, with maximum latitude occurring at 1800 to 2000 GMT and minimum latitude at 0800 to 1200 GMT. He suggests that the variation of low energy flux might be due to "wobbling" of the geomagnetic axis with respect to the solar wind direction, since the maximum latitude occurs when the angle between the geomagnetic axis and the sun-earth line is a minimum.

IV.5. Plasmapause and Troughs

The presence of a plasmapause, i.e., a sharp drop in electron number density at a radial distance of 2 to 6 earth radii above the equatorial region, was established by Carpenter[48] from whistler measurements, and by Gringauz[49] from particle measurements. Reber and Ellis[50] from cosmic ray, and Warren[51]

from topside sounding data reported significant depletions in the electron density at the peak of the F-layer near 50° geomagnetic latitude. Muldrew[25] showed that "troughs" in the electron density at the peak of the F-layer, are a persistent feature of the nighttime and mid- and high latitude ionosphere. The troughs are aligned in the magnetic east-west direction, and are usually a few degrees wide in north-south direction. The electron density in the main (the most southerly, or mid-latitude) trough is typically one-fourth that of the background density. The average location of the main trough during November 1962 to March 1963 is shown in Fig. 11[52]. The trough is generally masked by day time production; during magnetic storms it shifts toward the equator by about 2° per unit Kp[25,53,54]. Sharp et al[55] and Sharp[56] reported abrupt changes in ion concentration measurements, made on low altitude satellites, that are probably related to the troughs.

Muldrew[25] suggested that the main trough was an extension along magnetic field lines, of the whistler "knee". Subsequent work has further confirmed a close correlation between the two[54,57] but there are important differences. First, the decrease of N at the plasmapause is primarily in the vertical direction, whereas the troughs are observed in N_{max} F2 which occurs at practically constant heights above (and close to) the earth. Second, the electron density beyond the plasmapause does not appear to increase significantly, whereas north of the main trough, the density at the peak of the F-layer increases, often to values as great as those south of the trough, and other troughs are observed at higher latitudes. Third, the troughs are primarily nighttime phenomena, and are generally masked during the day, whereas the plasmapause can be observed at all times of day. Fourth, the

troughs occur in the height range of maximum production of ionization, whereas nearly all of the ionization present near the plasmapause must have been produced elsewhere, and have been diffused or otherwise transported over large distances. Fifth, although the magnetic L-shell along which the plasmapause and the trough are located agrees well during the night, during morning and afternoon the main trough appears to move to higher L-shells than the plasmapause (Fig. 11).

In Fig. 11, the plasmapause is from Carpenter's observations for July 1963[58], the trough from Muldrew's northern hemisphere winter 1962-63 data[25], and the two limits of open field lines are an estimate from the "splash" precipitation data presented by Hartz and Brice[42], and the theoretical limit given by Nishida[59].

Because of the different periods of observation the plasmapause and trough observations are not strictly comparable, but they are the most complete data available, and probably represent the gross features of the diurnal variations in position of the two phenomena. As Fig. 11 shows, the trough is located approximately along the boundary of the region of open field lines (i.e., the neutral points) when it is first observed in the early afternoon, but moves equatorward to a position about 10° from that boundary between 1500 and 2000 LMT. The return of the trough in the late morning to the limit of the open field lines cannot be followed because of its obscuration during the day; it shifts slowly toward higher latitudes between about 0100 and the time it becomes obscured, around 0700 LMT. Between 1900 and 0500 LMT the plasmapause and the trough positions are in good agreement, but the two appear to have inverse diurnal variations of position; the plasmapause moves poleward around 1700 LMT and equatorward about 0500 LMT.

IV.6. Electron Density Distribution Over the Polar Region During Quiet Periods

In general spatial and temporal variations of the distribution of electron density above the peak of the F-layer are much more regular in the latitude region below the main trough than in the higher latitude region, for both quiet and disturbed conditions[60] (Fig. 12). Nevertheless, several studies of the distribution in the high latitude regions have succeeded in isolating some persistent structures.

IV.6.1. N(h) Distributions Below 1000 Km

Nishida[59] produced "average" electron density contours on a geomagnetic latitude vs local time plot for quiet intervals of the autumn (northern hemosphere) 1962-63, as shown in Fig. 13. For this study he used a "mesh" 4° in longitude and 2 hrs in local time. The general features of the main trough and the decreased complexity at the higher heights can be seen from this figure. Unfortunately, some of the detail is lost in these figures because the N(h) data used (the DRTE N(h) data publications) tend to avoid some of the important but complex structures in the topside ionosphere, while emphasizing other phenomena. In particular, the data probably favour profiles in which the density at the satellite is substantial, and neglect some data in which the electron densities are very small. Nevertheless, the diagrams provide a useful picture of the polar quiet ionosphere. Figure 14 shows the variability of the data, defined by Nishida as the standard deviation divided by the average, for each mesh point, expressed as a percentage. It is of interest that the greatest variability occurred at 1000 km, and with the exception of the 0800 LT graph, occurred in the region of the splash boundary (Fig. 11).

Nishida[39,59] explained the plasmapause and the trough regions in terms of an "outward flow" model in which plasma is removed by the combined action of magnetospheric convection and plasma escape from the tail of the magnetosphere. In his model, ionization will be removed by upward flow along field lines that are open into the magnetospheric tail (i.e., within the cross-hatched region of Fig. 11). However, all field lines poleward of the plasmapause become open (i.e., are convected through the cross-hatched region of Fig. 11) at some time during the night, and in the process can dump ionization in proportion to the time they spend in the "open" region.

Chan and Colin[61] have recently prepared a massive study and review of the global morphology of the distribution of electron density above the peak of the F-layer (primarily for low and mid-latitudes), based on N(h) data from the Alouette I and II satellite. It is not possible here to present the results of that work; the reader is referred to it and to reference 60 for average and detailed contours respectively of electron density in the polar regions. Much of the remainder of this section is, of course, also reviewed in the Chan and Colin paper.

IV.6.2. Electron Density at 1000 km

Thomas et al[62] studied latitudinal electron density maxima (as opposed to the troughs of Muldrew) above the main trough. They found a density maximum immediately beyond the trough to be a persistent feature of the ionosphere below 1000 km, with maximum to trough density ratios of 25 to 1 a common occurrence. Although the diurnal variation of this maxima was not established, at about 1500 LMT it occurred at about 77° geomagnetic latitude, the location of the boundary of the open field lines. Thomas et al related

this maxima to that found at the peak of the F-layer by Duncan[63] from ground-based ionosonde data. Duncan showed that polar enhancements of foF2 were largely GMT controlled, with maximum ionization occurring at 1800 GMT in the north and 0600 GMT in the south, the time at which the angle between the geomagnetic axis and the sun-earth line is a minimum. He suggested that the enhancements were due to particle precipitation; Thomas et al[62] suggested that the maximum they observed was due to upward diffusion of ionization from the precipitation production region. Maehlum[47] found a similar GMT control of low energy electrons (50-1000 ev) and noted the possibility of a relation between the ionospheric maxima and the peak of low energy particle precipitation.

Sato and Colin[46] showed that at 1000 km high latitude ionization maxima (Fig. 15) generally occurred more frequently and had greater amplitude during the day than during the night, especially in winter, and that the amplitude of the maxima was greater in summer than in winter. They showed that the maxima did not occur uniformly over the high latitude region, but in three zones (Fig. 16), with the maxima in a particular zone related, but independent of those in the other zones. In zones I and III, the maxima occur most frequently during periods of high geomagnetic activity. In zone I the maxima occur most often at dawn and dusk, in zone II most frequently in daytime regardless of geomagnetic activity or season, and in zone III mainly at night. The boundaries of the three zones vary, depending upon magnetic local time, season and magnetic activity.

Zone II corresponds approximately to the auroral oval, i.e., to the region of splash precipitation given by Hartz and Brice (Fig. 11). The maxima previously found by Thomas, et al[62] occur within zone II. Sato and

Colin concluded that the electron density maxima were due to low energy electrons (E < 1 keV) precipitated from electron islands outside the trapped region into zone I, from an unstable trapped region close to the trapping boundary into zone II, and from stable trapped regions into zone III.

IV.6.3. N(h) Distributions Below 3000 km

The foregoing studies were, in general, for altitudes below 1000 km; Nelms and Lockwood[9] showed that at heights near 2000 km, N(h) profiles taken while approaching (and close to) the low latitude edge of the trough showed a successive decrease of scale height near 2000 km, whereas the distribution near 500 km remained approximately the same from record to record (Fig. 17). They also showed that at heights above 2400 km, the electron density was less than 300 to 500 electrons/cm^3 over a large area of the polar region (Fig. 18). The southern boundary of this low density region was found to agree in general with the location of the main trough. They interpreted the decrease in scale height and the presence of the extensive low density region at high heights as equivalent to a shift of the region of predominance of the O^+/H^+ mixture (i.e., the level at which the H^+ concentration became comparable with the O^+ concentration) to great heights in the vicinity of the trough and at latitudes greater than the trough.

IV.6.4. Electron Density at the Height of the Alouette II Satellite (500 to 3000 km)

The low density limit of the Nelms-Lockwood work was set by the sweep limit of the Alouette II sounder; Hagg[19], using the resonance beat method outlined in Section III, showed that electron densities in the low density region were very often less than 30 electrons/cm^3 and frequently were as low

as 8 to 15 electrons/cm^3. The interpretation that the very low electron densities are due to an upward shift of the H^+ distribution is supported by the data of Hoffman[22], who found that on several occasions when Hagg observed very low electron densities, the predominant ion, even near 3000 km, was O^+. In addition, Hoffman has observed upward streaming of H^+ ions at certain times in the polar regions[22,64].

Hagg found that densities less than 30 electrons/cm^3 were observed in the northern hemisphere throughout the region above 60° geomagnetic latitude at night and 65° geomagnetic during the day. Timleck and Nelms[20] used the Hagg method to study the occurrence of densities less than 100 electrons/cm^3 between December 1965 and February 1968 in both northern and southern hemispheres. They found that below 3000 km altitude the low densities were much more prevalent during winter than during summer; during the summer the low densities were observed only near the region of the main trough and only near midnight.

Figure 19 is a scatter diagram from the Timleck-Nelms study, showing the occurrence of densities less than 100 cm^{-3} as a function of geomagnetic latitude and local mean time for all of the Northern hemisphere data collected between December 1965 and December 1967 (note: it includes the data from the Hagg study). About 4.5% of the data are for $Kp \geq 4$. The dashed line in Fig. 19 is a crude estimate of the low latitude boundary of the low density region for relatively quiet conditions (i.e., about 4.5% of the data points are outside the dashed line). Although only an estimate, the real boundary is not likely to be significantly displaced from the one shown. The projection of the boundary down the field to the 300 km level, from an assumed height of 2800 km, is plotted on Fig. 11.

The separation of altitude, LMT and latitude effects in the low density data is difficult because of the high inclination eliptical orbit of Alouette II. However, Timleck and Nelms isolated a diurnal and sunspot cycle dependence of the minimum height at which electron density of 100 cm^{-3} occurred, as shown in Fig. 20. Because of the orbit and the fact that the low densities occur above about 60° geomagnetic latitude, the satellite was not in a position to establish the low height limit at times other than those shown in Fig. 20.

The densities less than 100 cm^{-3} occur at lower heights during the night than during the day, and there is a general tendency toward higher heights during most recent years. The exception, midnight to 0400 LMT, is thought[20] to be due to a seasonal effect overriding the diurnal effect; the 1965-66 data for these hours were collected during December whereas the 1967-68 data were collected during February. Two of the periods when no low electron densities were observed over the polar region, even though they were to be expected from immediately preceding and following data, were found to coincide with proton events observed by the IMP-F satellite.

Banks and Holzer[65] interpreted the Hagg[19] results, and Timleck and Nelms[20] interpreted their results in terms of the removal of light ions by upward flow in regions where the field lines are swept back into the tail of the magnetosphere. Banks and Holzer showed that essentially all of the thermal H^+ and He^+ ions created in the polar ionosphere can be accelerated away from the earth into the tail of the magnetosphere, but that the upward velocity of the O^+ ions, because of their greater mass, will be small for heights below a few thousand kilometers. Timleck and Nelms showed that the electron densities

observed in their regions of very low electron density were approximately what would be expected if the light ions were removed, leaving behind a relatively unaltered O^+ distribution. They explained the diurnal variation of the cut-off height for $N \leq 100/cm^3$ as due to daytime production (of O^+) raising the height at which $N = 100/cm^3$ occurs. The summertime absence of observations of $N \leq 100/cm^3$ below 3000 km, except for a few occurrences immediately above the main trough, they attributed to increased production during the time when much of the polar region is continually illuminated. They pointed out that the cut-off height would be expected to rise during times of disturbance or particle precipitation, either due to increased production or increased temperature.

IV.7. Electron Density Distributions Over the Polar Region During Disturbed Periods

Although this paper concentrates on the high latitude topside ionosphere, it is useful to introduce the subject of the disturbed ionosphere with a brief discussion of the general global behaviour. The relevant literature on this complex subject is extensive, so the following brief discussion is guaranteed to be incomplete; the reader is referred for more detail to references 45, 59, and 66-68 from which the present authors have drawn much of the following summary.

In general, ionospheric storms can be considered to be due to enhanced influx of energetic particles (from thermal to MEV) from the solar wind near the earth, and may be due to direct effects of the particles such as (ionization or heating of the upper atmosphere, or to indirect effects) such as distortion of the geomagnetic field (the geomagnetic storm), establishment of ring currents that cause ionization drifts, etc.

At the sudden commencement of a magnetic storm, the front (day-side) of the magnetosphere is compressed[69], and this increases both the electron density and the magnetic field in the topside ionosphere. This initial phase of the storm may last up to 10 hours. At the beginning of the main phase of the magnetic storm the magnetic field is inflated by energetic particles[70] that appear to be injected into trapped orbits near the plasmapause at late afternoon and evening longitudes. The decay of this enhanced particle belt may take several days.

The ionospheric storm effects are observed as changes (increases or decreases) of electron number density in various height and latitude regions, changes in electron and ion temperature, neutral and in composition, recombination rates, and transport velocities. All of these may vary independently in different height, latitude, seasonal and diurnal regimes, and may also have different storm time behaviour. In spite of this great complexity, it appears that some useful general patterns are now beginning to emerge[68].

At mid latitudes the beginning of the ionospheric storm on the day side of the earth is associated with the beginning of the main phase of the magnetic storm[71,72], rather than with the sudden commencement. However, on the night side the full ionospheric storm does not occur until the following day[73]. Gledhill et al[74] found that ionospheric storms invariably occurred when the flux level of precipitated electrons ($E > 40$ keV), measured in Alouette I, rose above 1.4×10^4 electrons/cm^2/sec, and that the storm lasted a time proportional to the time this critical flux was exceeded.

The major disturbances during an ionospheric storm are in the electron density in the D and F region, and in the ion and electron temperatures near

the peak of the F layer. At high latitudes the electron density in the D region is enhanced while at mid latitudes the total content[75,76] and the density at the peak of the F layer usually are first enhanced over about 24 hours (positive phase) and then depressed over a period of a few days (negative phase). However, the decrease in density at the peak precedes the decrease in total content by several hours[76], and occasionally, large systematic storm-time variations in topside total content occur that are not accompanied by significant or regular changes in the peak density or in the bottomside content[75]. At lower latitudes, the positive phase increases and the negative phase decreases until only the positive phase remains at the equator[77].

IV.7.1. Plasma Temperatures During Storms

Incoherent scatter measurements at mid-latitudes have been used to show that during the day the disturbed and quiet day electron temperatures in the F region below about 400 km appear to be about the same[78,79], whereas above 400 km the electron temperature is slightly higher on disturbed days. During the night, the disturbed time electron temperature is 300° to 600°K greater, and the ion temperature is slightly greater than in quiet times. The ion temperature below 400 km is greater, and above 400 km is slightly less on disturbed than on quiet days.

Willmore[80], using Ariel I data, found that between 0400 and 1200 km altitude electron density enhancements, and electron temperature decreases of about 180°K, were associated with geomagnetic storms, both at night and during the day. He attributed the temperature changes to increased collisional cooling due to the increased electron density.

Ondoh[67], from Alouette I data, found that during mild storms the electron density increased above 500 km height and decreased below at all local times. He concluded that the increase was due to expansion of the neutral atmosphere, which would lift the whole ionosphere, causing higher densities at high heights[81]. The decrease below 500 km he attributed to increased chemical losses. Like Willmore, he expected the enhanced electron density above 500 km to cause decreased temperature through additional collisional cooling. Decreased electron density in this region during severe storms should then allow the temperature to increase. Reddy et al[82] found a similar result at 640 km, by relating bottomside sounding data to probe data from Tiros 7, and also found that measured decreases in electron temperature were associated with the increases in density at 640 km. They also interpreted the storm-time enhancements as due to thermal expansion of the neutral gas lifting the whole ionosphere.

IV.7.2. N(h) Distributions During Storms

Nishida[59] investigated structures in the polar disturbed ionosphere, using Alouette I N(h) data. He constructed "deviation" contours, similar to his variability plots of Fig. 14, using the difference between the storm and average quiet day data, expressed as a percentage of the quiet day data. An example is given in Fig. 21, for the magnetic storm of 23 Sept. 1963, for Kp = 9^-. Regions of storm-time density reduction are shaded. Below 66°N geomagnetic at noon, and below 82°N geomagnetic at midnight the storm time ionosphere is enhanced above and depleted below 450 km. A general storm time depletion at all heights over the polar region is evident. Nishida showed that storm-time changes enhanced the high latitude peaks, often to as much as

five times their average value, and caused them to move several degrees south. He also found that the plasma was depleted at the pole and in the trough.

Nishida explained his results in terms of the number of field lines convected through the "open" tail region of the magnetosphere, and of heating of the magnetospheric plasma by the hot storm-time solar wind (i.e., the area and velocity of plasma exit). He pointed out that the plasma temperature increases toward the magnetopause[83], the temperature of the solar wind increases with increasing Kp[84,85], and more field lines are transported into the tail region[86] during storm than during quiet times. All of these would tend to increase the escape of plasma from the polar regions through the magnetospheric tail, leading to the observed reduction of electron density over the polar region. He also invoked lifting of the plasma due to heating to explain the increased density above and decreased density below 500 km at mid-latitudes.

Sato[66] constructed contours of the Nishida type for 20 disturbed passes of Alouette I for the low and mid-latitude regions. An example is shown in Fig. 22 for a typical disturbed nighttime pass. Regions of storm time density reduction are shaded. During the night, the topside ionosphere at geomagnetic latitudes below 40° in the north and 50° in the south was all enhanced. Since the main trough in the northern hemosphere moves equatorward about 2° per unit Kp during increased magnetic activity[52], the reductions at 45°N and 55°S are probably due to the trough.

Sato's results were similar to those of Ondoh[67] for the mid latitude region. (The reader is referred to the paper for Sato's low latitude results.) He found that each pass differed somewhat from the others but tentatively concluded that at mid latitudes

(1) the density was often enhanced in the upper region (near 1000 km) but decreased near the peak of the layer. Less often the reverse was true.

(2) The percentage variation was larger in the lower than in the upper topside ionosphere.

(3) The density was most often enhanced between 30° and 40° and reduced between 40° and 50° geomagnetic latitude. The enhancements occurred over wider ranges of latitudes and height in local summer and equinox than in winter.

He concluded that drift motion and ambipolar diffusion could not alone explain his mid-latitude storm-time observations, and suggested that lifting of the ionosphere due to thermal expansion might be involved.

Sato and Chan[45] extended the study of storm-time deviation contours of Sato[66] to cover 24 Alouette I passes over the north polar region. They found that above 60° invariant latitude the deviations from quiet day showed a strong dependence on magnetic local time as well as on latitude and height. Figure 23 summarizes the results of their study. Storm-time enhancements occur in two well defined regions above 80°N near dawn and dusk at low heights, with the rest of the region above 60°N, except for a small region near noon at 60°N, a region of electron density reduction.

At higher heights the regions of enhancement all expand, until at 1000 km the enhanced region covers a large portion of the day time region below 70° latitude and of the nighttime region above 80° latitude.

The Nishida[59] results (reduction over a large region near the geomagnetic pole) are explained by Sato and Chan as due to the fact that Nishida's data

was only in the noon-midnight local time plane (both authors used the same Alouette I data, so it is expected that their results will agree wherever they overlap). Sato and Chan also relate their results to the measurements of abnormally large electron peaks at 1000 km[62,46]. The distribution of peaks in winter for low and high magnetic activity[46] are shown in Fig. 24. On quiet days the peaks are confined to zone II (Fig. 16) on the day side, whereas on disturbed days, they spread over the whole region above 70°, although still concentrated on the day side. Although the evidence for a movement of the peaks to lower latitudes is not overwhelming, Sato and Chan note the tendency, and relate it to similar storm time behaviour of the auroral oval, which is thought to be due to the lowering of the precipitation latitudes of low energy electrons ($E < 1$ keV) during storms. They explain the presence during storms of peaks in the region above 80°N as due to precipitation of low energy electrons from the neutral sheet into the polar region. Thus they interpret the storm-time behaviour of the topside polar ionosphere as due to

(a) lowering of the particle precipitation latitude of low energy electrons.

(b) enhancement of the precipitating electron flux intensity at high latitudes.

The effect of (a) is to produce a reduction region (from the absence of particle precipitation), while the effect of (b) is to produce an enhancement region near the pole.

It will be noted that Figs. 23 and 24 are in a sense contradictory; since the peaks move to lower latitudes during storms, as shown in Fig. 24, there should be an enhancement region between 70° and 75° at 1500 to 1800 LMT and near 65° at 2000 to 2300 LMT. However, this amount of detail is probably not to be expected to survive the averaging processes used in producing Fig. 23.

Several authors[87-89,68] have studied the occurrence of large electron density decreases at the peak of the F2 layer in which the F1 layer became visible from the topside (the "G" condition). An example of an Alouette I pass during a severe storm, during which the G condition was observed[87,68] is shown in Fig. 25. Herzberg and Nelms[88] did not find a systematic pattern to the occurrence of G condition before and during the sudden commencement associated with the proton flare storm of 7 July 1966 (Fig. 26). Norton[89] concluded that the vertical drifts alone could not explain the G-condition data, and suggested that an increase of the loss rate by a factor of 16 over the quiet day values was required to fit the G condition data. The loss rate can be increased by increasing the N_2 or O_2 density or by increasing the rate coefficient for reactions of these molecules with O^+; Norton suggests that increased mixing might increase the neutral density sufficiently to explain the results, but favours rather an enhanced reaction[90] between vibrationally excited N_2 and O^+. Laboratory measurements of the reaction rate[91] indicate that at electron temperatures of 3000° to 4000°K the enhancement should be sufficient to explain the G condition observations data.

During the proton event of 7 July 1966, Herzberg and Nelms[88] also observed a series of vertical bands across the normal ionospheric reflection traces on Alouette II ionograms, which they called a Σ-condition, and interpreted as due to narrow (~ 2 km) vertical regions of electron density depletion, or "mini-troughs". This interpretation was supported by the plasma probe on Alouette II, which measured small scale electron density depletions at the time the Σ-condition was observed. The Σ-condition occurred at L values of about 11 (about 77° geomagnetic) before the sudden commencement, and about

6 (about 65° geomagnetic) afterward (Fig. 27). For the very limited data available, it was found to occur in coincidence with sudden changes in the intensity of energetic particles of energy greater than 35 keV, and only in conjunction with proton events. The note added in proof to their paper, in which they reported a Σ-condition for which no proton flare was reported was later found to be premature. The associated proton flare was later reported from satellite observations.

Norton and Marovich[92] obtained Alouette I and II topside sounder data in coincidence with visual observations of red arcs[93] (enhanced 6300 Å airglow) over the central USA (L values of ~ 3). The peak emission rate for red arcs occurs at heights of 350 to 450 km. They usually extend a few hundred km in altitude but a few thousand km in magnetic longitude. Red arcs move from high to mid latitudes during magnetic storms[94]. Norton and Marovich found that a major depression in topside electron density occurred over the region of the arc, and from scale height measurements, inferred that the plasma temperature and the ion mass within and above the arc were considerably greater than equatorward of it. They concluded that the electron density reduction was the main (mid latitude) trough. Recent explanations of 6300 Å airglow invoke collisional excitation of atomic oxygen by energetic electrons[95], which implies energetic electrons may play an important role in the production of the main trough, at least during storm conditions when red arcs are observed.

V. DISCUSSION

Much of the data from observations of the high latitude high altitude ionosphere can be characterized in terms of events and boundaries that are part

of the magnetospheric environment of the earth. The enhancements of electron density in the upper ionosphere, while apparently highly irregular in individual behaviour, occur in zones that are relatively well behaved, and that appear to be related to regions of particle precipitation. Observed reductions of electron density, on the other hand, appear to be related to regions of open field lines in the magnetosphere. The two regions, of course, overlap, so the overall picture tends to be complicated.

Axford and Hines[97] proposed a model in which viscious drag from the solar wind caused large scale convection of the plasma in the magnetospheric cavity beyond L shells of about 4 Re, and used the resulting convection patterns to explain a high latitude auroral phenomena. Their model has been extended by, among others, Nishida[39,59] and Brice[96], who use it to explain a number of ionospheric phenomena.

Both Nishida and Brice consider the plasmapause to be the boundary of the plasma that co-rotates with the earth, and the plasma beyond the plasmapause to be convected through the magnetosphere at some time during the diurnal rotation. However, a basic difference between the Nishida and the Brice models is that the former explained the decreased density in the region beyond the plasmapause as due to the convection of plasma of terrestrial origin out into the essentially open tail of the magnetosphere, whereas the latter considered the plasmapause as an equipotential boundary between the plasma of terrestrial origin (inside) and plasma that has migrated (or been convected) in from the solar wind. It now appears that the two models are not necessarily incompatible; the inward flow model is supported by observations of energetic (above a few eV) particle data and, as shown by Brice, agrees with the observations

of the ambient plasma, whereas the outward flow model appears to find its major support from the observations of the near-thermal plasma.

In the Nishida model, ionization will be removed along field lines that are open (i.e., within the cross-hatched region of Fig. 11), but all of the field lines polarward of the plasmapause become open (i.e., pass through the cross-hatched region of Fig. 11) some time during the day, and in the process can dump ionization in proportion to the time they spend in the open region. On the day side of the earth the boundary of the region of open field lines is also the locus of the neutral points, and along this boundary particles can directly penetrate the magnetosphere from interplanetary space. Field lines within the cross-hatched region are swept back in the nightside tail, and are also open and accessible to particles from the interplanetary medium. On the night side of the earth, the boundary of the region of open field lines is the locus of the neutral sheet, and corresponds to the region in which energetic particles from the magnetospheric tail can obtain direct access.

From either model, it appears that there are two important boundaries in the magnetosphere; the plasmapause (below which the field lines are simply connected to the conjugate hemisphere) and the boundary of the open field lines, above (in latitude) which the field lines are open into the magnetospheric tail (other boundaries are, of course, observed at other latitudes). It is instructive here to consider further the relation of certain high latitude ionospheric data to the plasmapause and the region of open field lines.

The height distribution of electron density in the high ionosphere is governed primarily by electron production (which occurs predominantly at

low heights) and loss, temperature, ionic mass (gravitational forces), and the earth's magnetic field. In regions where the field lines are simply connected to the conjugate hemisphere, the field acts as a container to the ionization; light ions that have sufficient energy will not readily escape, but will simply travel along the field and may even reach the opposite hemisphere. Thus a general equilibrium is built up along the field, and an increase in production or temperature simply places more ionization at high heights in the "container", forcing the different ion distributions to adjust themselves so that a new pressure balance is obtained. In the polar regions the field lines are swept back into the tail of the magnetosphere, and the light ions can expand into a very large (essentially open) volume. Thus a given temperature of the ion gas will have a very different effect in the mid-latitude and high-latitude regions.

Bauer[40], in a comprehensive study of diffusive equilibrium as applied to the topside ionosphere shows that diffusive equilibrium, which is a consequence of a Maxwellian velocity distribution of particles and therefore is dependent on collisions, may break down at latitudes beyond the trough (beyond the plasmapause). In these regions, where the local electron density can be very low, a "collisionless" or ion-exosphere distribution is required, as derived by Eviater, et al[98]. Figure 27 compares the diffusive equilibrium and the collisionless models, and illustrates the very rapid decrease of density with altitude that would be expected in the collisionless region. Experimental data from knee whistlers are found to correspond to the R^{-4} density distribution outside the plasmapause[100], i.e., approximate the collisionless distribution.

Banks and Holzer[65] have shown that essentially all of the H^+ and He^+ ions created in the polar ionosphere can be accelerated away from the earth into the tail of the magnetosphere, but because of its greater mass, the upward velocity of O^+ will be small for heights below a few thousand kilometers. The process of removal of the light ions over the polar region (the "polar wind" of Axford[98]) is, of course, a dynamic one, and during periods of ionization production may well be obscured. Also, particle precipitation and direct coupling of energy into the polar region will often complicate the picture. The models of Nishida and Banks and Holzer and of Bauer are essentially two different views of the way in which the absence of a closed magnetic field container results in a markedly different flow and distribution of ionization.

The picture presented by the "outward flow" models is, of course oversimplified, just as a picture that relies entirely upon particle precipitation to explain the structures observed in polar ionosphere is probably oversimplified. A combination of the two, however, may provide a reasonably accurate model. We know that there is particle precipitation, that these particles will produce ionization, and that low energy particles will ionize in the upper ionosphere. Also, we know that there are extensive areas of very low electron densities at a few thousand km above the polar regions, that there are troughs that extend to the peak of the F layer, that very few light ions are found, even at 3000 km height in these very low density regions, and that outward flow of light ions has been observed in the polar regions.

The main trough appears to be at the locus of the lowest latitude region along which ionization can be readily removed from the peak of the F layer. If this removal is by upward acceleration of ionization, as suggested

by Nishida and by Banks and Holzer, production of ionization during the day is probably faster than the removal process, which explains why the trough does not appear as a well defined structure during the day. In the afternoon, as production decreases, the trough at the peak of the layer appears, first along those field lines that are open into the tail of the magnetosphere, and later at lower latitudes, down to the limit of the convective region (i.e., the limit of the plasmapause) during most of the night. As suggested by Nishida, if no inward particle precipitation were present during the night the whole of the region from the plasmapause boundary to the pole might be one large "trough", with perhaps a greater depletion of ionization over the region of open field lines than between that region and the plasmapause boundary. The peaks of ionization at latitudes above the main trough may therefore be due to ionization produced by particle precipitation, either from trapped orbits (the"drizzle" precipitation of Hartz and Brice) or from particles that have entered the region along the open tail from the interplanetary medium. Also, one might expect that as one moved upward away from the main region of ionospheric production, that the daytime production would have less apparent effect, and the trough would be observable throughout the day. Since energetic particle precipitation causes ionization predominantly at low heights,at sufficiently great heights, the large trough over the whole of the convective region might be expected to be revealed, This is, of course, what is observed as is shown by the Alouette high latitude low density region (Fig. 13) and, even more strikingly, by the observations of electron density less than 100 cm^{-3} over much of the polar region above about 2000 km altitude[19,20] (Fig. 19).

Thus the model that we appear to require over the polar regions is one in which there is simultaneously a continual upward flow of near thermal ions (primarily H^+ and He^+) and electrons along the field, to be convected or dumped directly out the tail of the magnetosphere, and a (probably more sporadic) inward flow of low energy energetic particles from the solar wind into the tail of the magnetosphere (or through the neutral points) and down along the field into the ionosphere. As well, there will, of course be the flow of energetic particles into trapped orbits and precipitation from these trapped "belts" into the lower ionosphere.

It appears that the crucial measurements to be made at the present time are high altitude measurements of the flow of low energy (thermal to a few keV) particles, in both the upward and downward directions, along with the distribution of temperature of the ambient plasma.

ACKNOWLEDGEMENTS

The authors are indebted to P.L. Timleck for the use of Fig. 19 and to D.B. Muldrew for many helpful suggestions, particularly with reference to Fig. 11, which is along the lines of a similar figure from an unpublished paper by Muldrew. The authors have drawn liberally from review papers by K.L. Chan and L. Colin, D.H. Jelly and L.E. Petrie, D.B. Muldrew, and E.S. Warren, references 61, 52, 15 and 68, and wish to express their gratitude to those authors for access to pre-publication copies of the papers.

References

1. C.A. Franklin and M. Maclean, "The Design of Swept Frequency Topside Sounders", Proc. IEEE, in Press, June 1969.
2. E.L. Hagg, E.J. Hewens, and G.L. Nelms, "Interpretation of Topside Sounder Ionograms", Proc. IEEE, in Press, June 1969.
3. G.E.K. Lockwood, "Plasma and Cyclotron Spike Phenomena Observed in Top-Side Ionograms", Can. J. Phys., 41, p. 190, 1963.
4. W. Calvert and G.B. Goe, "Plasma Resonances in the Upper Ionosphere", J.G.R., 68, p. 6113, 1963.
5. F.D. Green, "Signals with Resonance Characteristics at Harmonics of the Plasma and Upper Hybrid Frequency Produced by the Alouette Satellites", in Press.
6. E.S. Warren and E.L. Hagg, "Observation of Electrostatic Resonances of the Ionospheric Plasma", Nature, 220, p. 466, November 1968.
7. E.L. Hagg and D.B. Muldrew, "A Novel Spike Observed on Alouette II Ionograms", Proc. Advanced Study Institute on Plasma Waves in Space and in the Laboratory Røros, Norway, 1968.
8. R.E. Barrington and T.R. Hartz, "Satellite Ionosonde Records: Resonances Below the Cyclotron Frequency", Science, 160, p. 181, April 1968.
9. G.L. Nelms and G.E.K. Lockwood, "Early Results from the Topside Sounder in the Alouette II Satellite", Space Research VII, North Holland Publishing Company, Amsterdam, p. 604, 1967.
10. E.L. Hagg, "Remote Cyclotron Resonance Phenomenon Observed by the Alouette Satellite", Nature, 210, p. 927, 1966.
11. D.B. Muldrew, "Delayed Cyclotron Pulse Generation in the Topside Ionosphere Deduced from Alouette I Data", Nature, 210, p. 471, 1966.

12. D.B. Muldrew and E.L. Hagg, "A Novel Ionospheric Cyclotron Resonance Phenomenon Observed on Alouette I Data", Can. J. Phys., 44, p. 925, 1966.

13. D.B. Muldrew, "Delayed Generation of an Electromagnetic Pulse in the Topside Ionosphere", J.G.R., 72, p. 3777, 1967.

14. D.B. Muldrew and E.L. Hagg, "Stimulation of Ionospheric-Resonance Echoes by the Alouette II Satellite", Proc. Advanced Study Institute on Plasma Waves in Space and in the Laboratory, Røros, Norway, 1968.

15. D.B. Muldrew, "Non-Vertical Propagation and Delayed-Echo Generation Observed by the Topside Sounders", Proc. IEEE, in Press, June 1969.

16. J.W. King and D.M. Preece, "Observations of Proton Gyro-Effects in the Topside Ionosphere", J. Atmos. Terrest. Phys., 29, p. 1387, 1967.

17. P. Graff, Compt. Rendu, 265, p. 618, 1967.

18. T. Ondoh, Private Communication.

19. E.L. Hagg, "Electron Densities of 8-100 Electrons cm^{-3} Deduced from Alouette II High Latitude Ionograms", Can. J. Phys., 45, p. 27, 1967.

20. P.L. Timleck and G.L. Nelms, "Electron Densities Less than 100 cm^{-3} in the Topside Ionosphere", Proc. IEEE, in Press, June 1969.

21. L.H. Brace and J.A. Findlay, "Comparison of Cylindrical Probes on Alouette II and Explorer XXXI", Proc. IEEE, in Press, June 1969.

22. J. Hoffman, "The Ion-Mass Spectrometer on Explorer XXXI Satellite", Proc. IEEE, in Press, June 1969.

23. D.B. Muldrew, Private Communication.

24. W. Calvert and C.W. Schmid, "Spread-F Observations by the Alouette Topside Sounder Satellite", J.G.R., 69, p. 1839, 1964.

25. D.B. Muldrew, "F-Layer Ionization Troughs Deduced from Alouette Data", J.G.R., 70, p. 2635, 1965.

26. L.E. Petrie, "Preliminary Results on Mid and High Latitude Topside Spread F", Spread F and Its Effects Upon Radio Wave Propagation and Communications, Edited by P. Newman, Technivision Press, Maidenhead, England, p. 67, 1966.

27. W. Calvert and J.M. Warnock, "Ionospheric Irregularities Observed by Topside Sounders", Proc. IEEE, in Press, June 1969.

28. G.E.K. Lockwood and L.E. Petrie, "Low Latitude Field Aligned Ionization Observed by the Alouette Topside Sounder", Planet. Space Sci., 11, p. 327, 1963.

29. D.B. Muldrew, "Radio Propagation Along Magnetic Field-Aligned Sheets of Ionization Observed by the Alouette Topside Sounder", J.G.R., 68, p. 5355, 1963.

30. B.T. Loftus, T.E. VanZandt and W. Calvert, "Observations of Conjugate Ducting by the Fixed-Frequency Topside-Sounder Satellite", Ann. de Geophys., 22, p. 530, 1966.

31. D.B. Muldrew, "Medium Frequency Conjugate Echoes Observed on Topside-Sounder Data", Can. J. Phys., 45, p. 3935, 1967.

32. P.L. Dyson, "Magnetic Field-Aligned Irregularities at Mid-Geomagnetic Latitudes", J. Atmos. Terrest. Phys., 29, p. 857, 1967.

33. J. Ramasastry, J. Walsh and J.R. Herman, "Research on Field-Aligned Propagation of HF Radiowaves using Alouette 2 Topside Sounder Data and Digital Ray-Tracing Techniques", Proc. AGARD/EPC XIVth Symposium "Scatter Propagation of Radio Waves", Oslo, 1968.

34. M.L.V. Pitteway and R. Cohen, "A Waveguide Interpretation of 'Temperate-Latitude Spread F' on Equatorial Ionograms", J.G.R., 66, p. 3141, 1961.

35. W. Calvert and R. Cohen, "The Interpretation and Synthesis of Certain Spread-F Configurations Appearing on Equatorial Ionograms", J.G.R., 66, p. 3125, 1961.

36. L. E. Petrie, "Topside Spread Echoes", Can. J. Phys., 41, p. 194, 1963.
37. R. J. Gallet, Aerodynamical Mechanisms Producing Electron Density Fluctuations in Turbulent Ionized Layers", Proc. IRE 43, N10 p. 1240, 1955.
38. G. Renau, "Theory of Spread F Based on Aspect Sensitive Backscatter Echoes",J.G.R., 65, N 8 p. 2269, 1960.
39. A. Nishida, "Formation of a Plasmapause, or Magnetospheric Plasma Knee by Combined Action of Magnetospheric Convection and Plasma Escape From the Tail", J.G.R., 71, p. 5669, 1966.
40. S. J. Bauer, "Diffusive Equilibrium in the Topside Ionosphere", Proc. IEEE in Press, June 1969.
41. I.B. McDiarmid, and J.R. Burrows, "Local Time Asymmetries in the High-Latitude Boundary of the Outer Radiation Zone for the Different Electron Energies", Can.J. Phys., p.49057, 46, 1968.
42. T.R. Hartz and N.M. Brice, "The General Pattern of Auroral Particle Precipitation", Planet.Space Sci. 15, p. 301, 1967.
43. B.J. O'Brien, "High-Latitude Geophysical Studies with Satellite Injun 3: Precipitation of Electrons into the Atmosphere", J.G.R., 69, p. 13, 1964.
44. I.B. McDiarmid and M.D. Wilson, "Dependence of the High Latitude Electron (E>35 keV) Boundary on the Orientation of the Geomagnetic Axis", J.G.R., 73, p. 7237, 1968.
45. T. Sato and K.L. Chan, "Storm Time Variations of Electron Concentration in the Polar Topside Ionosphere", J.G.R., In Press May, 1969.
46. T. Sato and L. Colin, "Morphology of Electron Density Enhancement at a Height of 1000 km at Polar Latitudes", J.G.R. In press May, 1969.
47. B.N. Maehlum, "Universal-Time Control of the Low-Engergy Electron Fluxes in the Polar Regions", J.G.R., 73, p. 3459, 1968/
48. D.L. Carpenter, "Whistler Evidence of a 'knee' in the Magnetospheric Ionization Density Profile", J.G.R., 68, p. 1675, 1963.
49. K.I. Gringauz, "The Structure of the Ionized Gas Envelope of Earth From Direct Measurements in the USSR of Local Charged Particle Concentrations", Planet Space Sci., 11, p. 281, 1963.

50. G. Reber, and G.R. Ellis, "Cosmic Radio-Frequency Radiation Near One Megacycle", J.G.R., 61, p. 1, 1956.

51. E.S. Warren, "Some Preliminary Results of Souding of the Topside of the Ionosphere by Radio Pulses From a Satellite", Nature, 197, p. 636, 1963.

52. D.H. Jelly and L.E. Petrie, "High-Latitude Ionosphere" Proc. IEEE, In Press, June, 1969.

53. L. Liszka, "The High-Latitude Trough in Ionospheric Electron Content", J. Atmos. Terr. Phys., 29, p. 1243, 1967.

54. M.J. Rycroft, and J.O. Thomas, "The Magnetospheric Plasmapause and the Electron Density Trough at the Alouette I Orbit", submitted to Planetary and Space Sci.

55. G.W. Sharp, T.J. Crowther, and C.W. Gilbreth, "Some Recent Ion Concentration Measurements Obtained from a Polar-orbiting and Satellite", (abstract), Trans. Am. Geophys. Union, 45, p. 87, 1964.

56. G.W. Sharp, "Midlatitude Trough in the Night Ionosphere", J.G.R., 71, p. 1345, 1966.

57. J.O. Thomas and M.K. Andrews, "Transpolar Exospheric Plasma", J.G.R., 73, p. 7407, 1968.

58. D.L. Carpenter, "Whistler Studies of the Plasmapause in the Magnetosphere", J.G.R., 71, p. 693, 1966.

59. A. Nishida, "Average Structure and Storm-Time Change of the Polar Topside Ionosphere at Sunspot Minimum", J.G.R., 72, p. 6051, 1967.

60. G.L. Nelms, "Seasonal Diurnal Variations of the Distribution of Electron Density in the Topside of the Ionosphere", Electron Density Profiles in the Ionosphere and Exosphere, North-Holland Publishing Company, 1966.

61. K.L. Chan and L. Colin, "Global Electron Density Distributions From Topside Soundings", Proc. IEEE, In Press, June, 1969.

62. J.O. Thomas, M.J. Rycroft, L.Colin and K.L. Chan, "The Topside Ionosphere, II," from Electron Density Profiles in Ionosphere and Exosphere, ed. J. Frihagen, (North Holland Publishing Co., Amsterdam), p. 322, 1966.

63. R.A. Duncan, "Universal-Time Control of the Arctic and Antarctic F-region", J.G.R., 67, p. 1823, 1962.

64. J. Hoffman, "Ion Composition Measurements in the Polar Region From the Explorer XXXI Satellite", Trans. Am. Geophys. Union, 49, p. 253, 1968.

65. P.M. Banks and T.E. Holzer, "The Polar Wind", J.G.R., 73, p. 6855, 1968.

66. T. Sato, "Electron Concentration Variations in the Topside Ionosphere Between 60° N and 60° S Geomagnetic Latitude Associated with Geomagnetic Disturbances", J.G.R., 73, p. 6225, 1968.

67. T.Ondoh, "Morphology of Disturbed Topside Ionosphere for 1962-1964", J. Radio Res. Labs., Japan, 14, p. 267, 1967.

68. E.S. Warren, "The Topside Ionosphere During Geomagnetic Storms", Proc. IEEE, In Press, June, 1969.

69. S.J. Bauer and B.V. Krishnamurthy, "Topside Ionsophere Behaviour During A Magnetic Storm", Plant. Space Sci , 16, p. 653, 1968.

70. L.J. Cahill, "Inflation of the Inner Magnetosphere During A Magnetic Storm", J.G.R., 71, p. 4505, 1966.

71. R.P.W. Lewis and D.H. McIntosh, "Geomagnetic and Ionospheric Relationships", J Atmos. Terr. Phys., 4, p. 44, 1953.

72. L. Thomas and F.H. Venables, "The Onset of the F-Region Disturbances at Middle Latitudes During Magnetic Storms", J. Atoms. Terr. Phys., 28, p. 599, 1966.

73. J.A. Ratcliffe and K. Weekes, "The Ionosphere", in Physics of the Upper Atmosphere, edited by J.A. Ratcliffe, Academic Press, London, 1960.

74. J.A. Gledhill, D.G. Torr, and M.R. Torr, "Ionospheric Disturbance and Electron Precipitation from the Outer Radiation Belt", J.G.R., 72, p. 209, 1967.

75. J.E. Titheridge and M.K. Andrews, "Changes in the Topside Ionosphere During a Large Magnetic Storm", Planet. Space Sci., 15, p. 1157, 1967.

76. F.H. Hibberd and W.J. Ross, "Variations in Total Electron Content and Other Ionospheric Parameters Associated with Magnetic Storms", J.G.R., 72, p. 5331, 1967.

77. E.V. Appleton and W.R. Piggott, "The Morphology of Storms in the F2 Layer of the Ionosphere", J. Atmos. Terr. Phys., 2, p. 236, 1952.

78. J.V. Evans, "Midlatitudes Ionospheric Temperatures on Magnetically Quiet and Disturbed Days", J.G.R., 70, p. 2726, 1965.

79. P.B. Rao, "Electron Concentrations and Electron and Ion Temperatures in the F Region for Magnetically Quiet and Disturbed Conditions", J.G.R., 72, p. 5331, 1967.

80. A.P. Willmore, "Electron Temperature of the Upper F-Region", Proc. Roy. Soc., A 286, p. 537, 1965.

81. O.K. Garriott and H. Rishbeth, "Effects of Temperature Changes on the Electron Density Profile in the F2 Layer", Planet. Space Sci., 11, p. 587, 1963.

82. B.M. Reddy, L.H. Brace, and J.A. Findlay, "The Ionosphere at 640 Kilometers on Quiet and Disturbed Days", J.G.R., 72, 2709, 1967.

83. G.P. Serbu, and E.J.R. Maier, "Low-Energy Electrons Measured in IMP 2", J.G.R., 71, p. 3755, 1966.

84. C.W. Snyder, M. Neugebauer, and U.R. Rao, "The Solar Wind Velocity and Its Correlation with Cosmic-Ray Variations and with Solar and Geomagnetic Activity", J.G.R., 68, p. 6361, 1963.

85. M. Neugebauer, and C.W. Snyder, "Mariner 2 Observations of the Solar Wind, 1, Average Properties", J.G.R., 71, p. 4469, 1966.

86. K.W. Behannon, and N.F. Ness, "Magnetic Storms in the Earth's Magnetic Tail", J.G.R., 71, p. 2327, 1966.

87. G.L. Nelms and E.S. Warren, "Some Irregular Variations of the Electron Density in the Topside of the Ionosphere", Space Research V, p. 637, 1965, North-Holland Publishing Company, Amsterdam.

88. L. Herzberg and G.L. Nelms, "Ionospheric Conditions Following the Proton Flare of 7 July 1966 as Deduced from Topside Soundings", Annals of IQSY, 3, p. 572, 1969.

89. R.B. Norton, "The Mid-latitude F Region During a Severe Ionospheric Storm", Proc. IEEE, in Press, June 1969.

90. L. Thomas, and R.B. Norton, "Possible Importance of Internal Excitation in Ion-Molecule Reactions in the F Region", J.G.R., 71, p. 227, 1966.

91. A.L. Schmeltekopf, F.C. Fehsenfeld, G.I. Gilman, and E.E. Ferguson, "Reaction of Atomic Oxygen Ions with Vibrationally Excited Nitrogen Molecules", Planet. Space Sci., 15, p. 401, 1967.

92. R.B. Norton and E. Marovich, "Alouette Observations Taken During a Mid-latitude Red Arc", Proc. IEEE, in Press, June 1969.

93. D. Barbier, "L'Arc Auroral Stable", Ann. Geophys., 14, p. 334, 1958.

94. F.E. Roach and J.R. Roach, "Stable 6300 Å Auroral Arcs in Mid-latitudes", Planet. Space Sci., 11, p. 523, 1963.

95. James C.G. Walker and M.H. Rees, "Excitation of Stable Auroral Red Arcs at Sub-auroral Latitudes" (in press 1968).

96. N.M. Brice, "Bulk Motion of the Magnetosphere", J.G.R., 72, p. 5193, 1967.

97. W.I. Axford and C.O. Hines, "A Unifying Theory of High-latitude Geophysical Phenomena and Geomagnetic Storms", Can. J. Phys., 39, p. 1433, 1961.

98. W.I. Axford, "The Polar Wind and the Terrestrial Helium Budget", J.G.R., 73, p. 21, 1968.

99. A. Eviatar, A.M. Lenchek and S.F. Singer, "Distribution of Density in an Ion-Exosphere of a Non-rotating Planet", Phys. of Fluids, 7, p. 1775, 1964.

100. J.J. Angerami and D.L. Carpenter, "Whistler Studies of the Plasmapause in the Magnetosphere 2; Electron Density and Total Tube Electron Content Near the Knee in Magnetospheric Ionization", J.G.R., 71, p. 711, 1966.

101. L. A. Frank, p. 271
102. E.W. Hones, p. 392
} "Physics of the Magnetosphere" Reidel Pub. Co. 1968

FIGURE CAPTIONS

Fig. 1: Alouette II ionogram illustrating the Z, O, and X-wave cut-offs, the Z-wave infinity, O and X wave penetration frequencies and various resonance spikes, including an apparent resonance spike labelled $f_T - f_N$. (From Hagg, Hewens and Nelms[2])

Fig. 2: An Alouette II ionogram illustrating the floating spike ($\frac{f_T}{2} \simeq f_N - f_H$), the f_D and the f_Q spikes. (From Hagg, Hewens and Nelms[2])

Fig. 3: An Alouette II ionogram showing the $2f_T$ and the remote resonance. (From Hagg, Hewens and Nelms[2])

Fig. 4: An Alouette II ionogram showing ionospheric resonance echoes at 1.98 MHz at apparent ranges less than 1200 km and greater than 4000 km. (From Muldrew and Hagg[14])

Fig. 5: An Alouette II ionogram illustrating the proton gyro-resonance identified by Ondoh[18].

Fig. 6: An Alouette II ionogram illustrating resonance beats on the combined f_T and f_H resonances. (After Hagg[19])

Fig. 6a: An ISIS-I ionogram taken in the mixed mode of sounding. The sounder transmitter was maintained at a fixed frequency of 0.833 MHz (f_{Tx})while the receiver was swept through the normal sweep range.

Fig. 6b: As for Fig. 6a, except that the sounder was switched to the normal sounding mode at 3.0 MHz.

Fig. 7: Alouette I ionogram with a spread trace between 200 and 300 km apparent range and 2.5 and 3.5 MHz resulting from echoes scattered from a high-latitude field-aligned irregularity. (After Petrie[36])

Fig. 8: Alouette I ionogram with a spread trace between 2.5 and 3.5 MHz resulting from echoes scattered from a low-latitude field-aligned irregularity. (After Lockwood and Petrie[28])

Fig. 9a: An ISIS-I ionogram recorded when the satellite was just outside a region of equatorial field-aligned irregularities.

Fig. 9b: An ISIS-I ionogram recorded when the satellite was within a region of equatorial field-aligned irregularities.

Fig. 10: An idealized representation of the two main zones of auroral particle precipitation (northern hemisphere). Average intensity of influx is indicated approximately by the density of the symbols. Coordinates are geomagnetic latitude and geomagnetic time. "Splash" precipitation is represented by triangles, "drizzle" precipitation by dots. (From Hartz and Brice[42]) Added to the Hartz-Brice diagram are a line estimate of the "splash" boundary (solid) and the boundary of the closed field region as given by McDiarmid and Wilson[44], from particle measurements (dashed).

Fig. 11: A local time vs. geomagnetic latitude plot of the location of the main trough (Muldrew), the equatorward limit of the region of electron density less than 100 el/cm^3 (Timleck and Nelms), the plasmapause (Carpenter), and experimental and theoretical determinations of the limit of the region of open field lines (McDiarmid and Wilson, and Nishida). All curves are projected to a height of 300 km.

Fig. 12: The contours of constant plasma frequency (electron density) as a function of height and geographic latitude for two passes in which Alouette II was near apogee over the north polar region. (from Nelms and Lockwood[9])

Fig. 13: The distribution of the average density in autumn at 950, 600, and 350 km levels. The average is obtained from the Alouette I profiles recorded in geomagnetically quiet intervals in autumn 1962 and 1963. (from Nishida[59])

Fig. 14: Meridianal distribution of the variability in 0800, 1200, 1800, and 2400 meridians from Alouette I data. Variability is derived by dividing, in each mesh point, standard deviation by average, and is expressed in the unit of per cent. (from Nishida[59])

Fig. 15: Electron density variation with two large enhancement peaks for seven successive Alouette I passes. Numbers at the top and bottom represent geographic latitudes and numbers under the reference levels indicate invariant latitudes. (from Sato and Colin[46])

Fig. 16a,b: Schematic representation of three zones, Zone I, II, and III, where peaks of electron density enhancements appear on disturbed days in winter (a) and summer (b). This zoning is only qualitative. Dotted shading areas show highly speculative zones, owing to rare occurrence of the enhancement in those zones. (from Sato and Colin[46])

Fig. 17: The N(h) profiles calculated from Alouette II ionograms recorded near the 75°W meridian and 00 LMT.(from Nelms and Lockwood[9])

Fig. 18: A polar plot of electron density at the height of the Alouette II satellite. The heavy and light lines indicate densities of greater and less than 500 electrons/cm^3 respectively for 18 passes taken between 1-15 December 1965. The planetary magnetic index Kp was less than 4 for the data shown. The location of the main trough found by Muldrew on 24 October 1962 (Kp = 4) at a comparable local time, is shown as a dashed line. (from Nelms and Lockwood[9])

Fig. 19: Occurrence of electron densities $\leq$ 100 cm^{-3}, observed on Alouette II ionograms, plotted against geomagnetic latitude (northern hemisphere) and local time for Dec 66 to Feb 67 and Dec 67 to Feb 68. The broken line indicates the approximate boundary for undisturbed conditions. (from Timleck)

Fig. 20: Low altitude cut-off of occurrence of electron densities ≤ 100 cm^{-3}, for the northern hemosphere winter from Alouette II data. The circled points indicate the lowest height at which low densities were observed. Data are not available to establish the low-altitude cut-off at times other than those shown here. (from Timleck & Nelms[20])

Fig. 21: Alouette I distribution of the relative deviation S $S = (n - N)/N$ of the electron concentration from the average value for 0035-0053, September 23, 1963, Kp = 9-, where n and N are the disturbed and quiet day distributions respectively. The region where the density is less than the average quiet interval value is shown by hatching. (from Nishida[59])

Fig. 22 Alouette I profiles of electron density variations in the topside ionosphere during geomagnetic disturbances in the nighttime. Shaded parts represent reduction of the electron density and non-shaded parts indicate enhancement or no variation. Solid lines show isopleths of the enhancement or reduction rates in percentage. (from Sato[66])

Fig. 23 Alouette I storm-time electron concentration variations at (a) 1000 km, (b) 600 km and (c) 300 km against invariant latitude and magnetic time in polar coordinate. Shaded areas represent electron concentration reduction and white areas, enhancement. (from Sato and Chan[45])

Fig. 24 Distribution of electron concentration enhancement peaks against invariant latitude and magnetic local time in the polar region at a height of 1000 km (from Alouette I) on (a) quiet and (b) disturbed days in winter. (after Sato and Colin[46])

Fig. 25 A cross section of the topside ionosphere from 180° to 37°W longitude during the occurrence of a G condition in the ionosphere. (from Warren[68])

Fig. 26 Geographical distribution after the solar proton flare of July 7, 1966, of (a) the G condition, (b) the Σ condition. (from Herzberg and Nelms[88] using Alouette I and II data)

Fig. 27 Plasma density distributions along a magnetic field line, whose apex in the equatorial plane is at $L = 5R_e$, are shown for a diffusive equilibrium, and a collisionless or ion-exosphere model, as well as for R^{-3} and R^{-4} power law models. The power law distributions are often employed for empirical models of the whistler medium. (from Bauer[40])

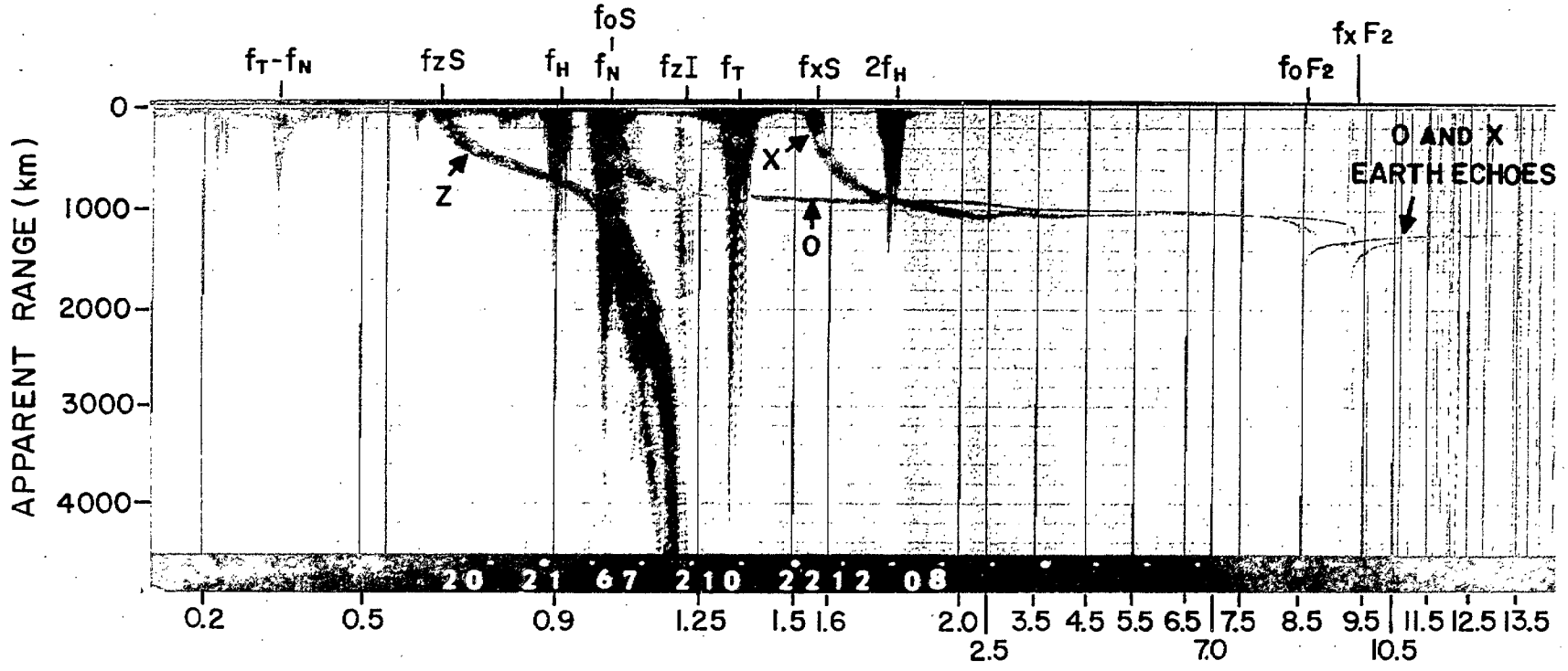

29 JULY 1967 2212/08 GMT (29.5°S, 160.5°E)
SATELLITE HEIGHT 1154 km

Fig 1

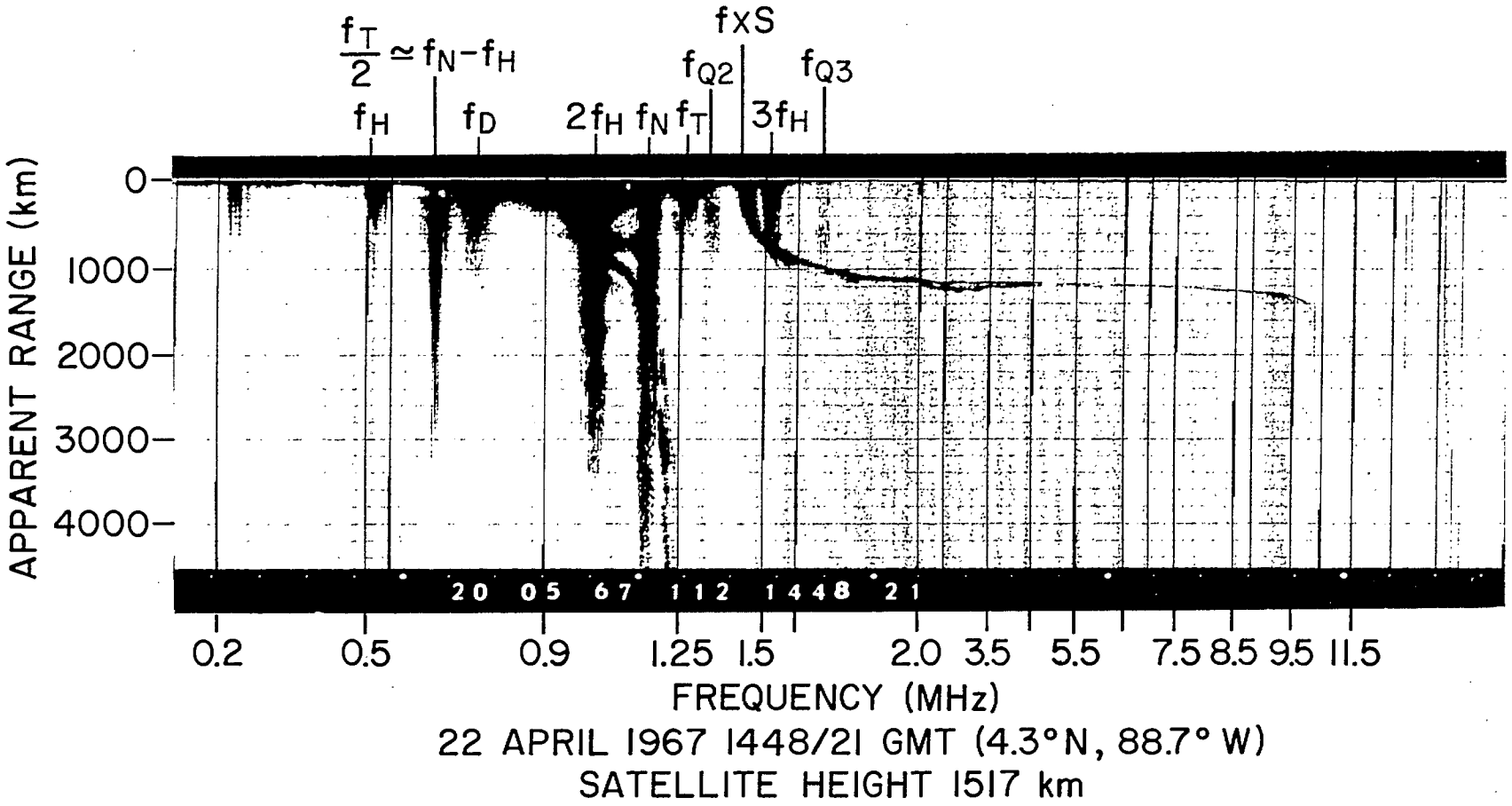

22 APRIL 1967 1448/21 GMT (4.3°N, 88.7° W)
SATELLITE HEIGHT 1517 km

FIG 3

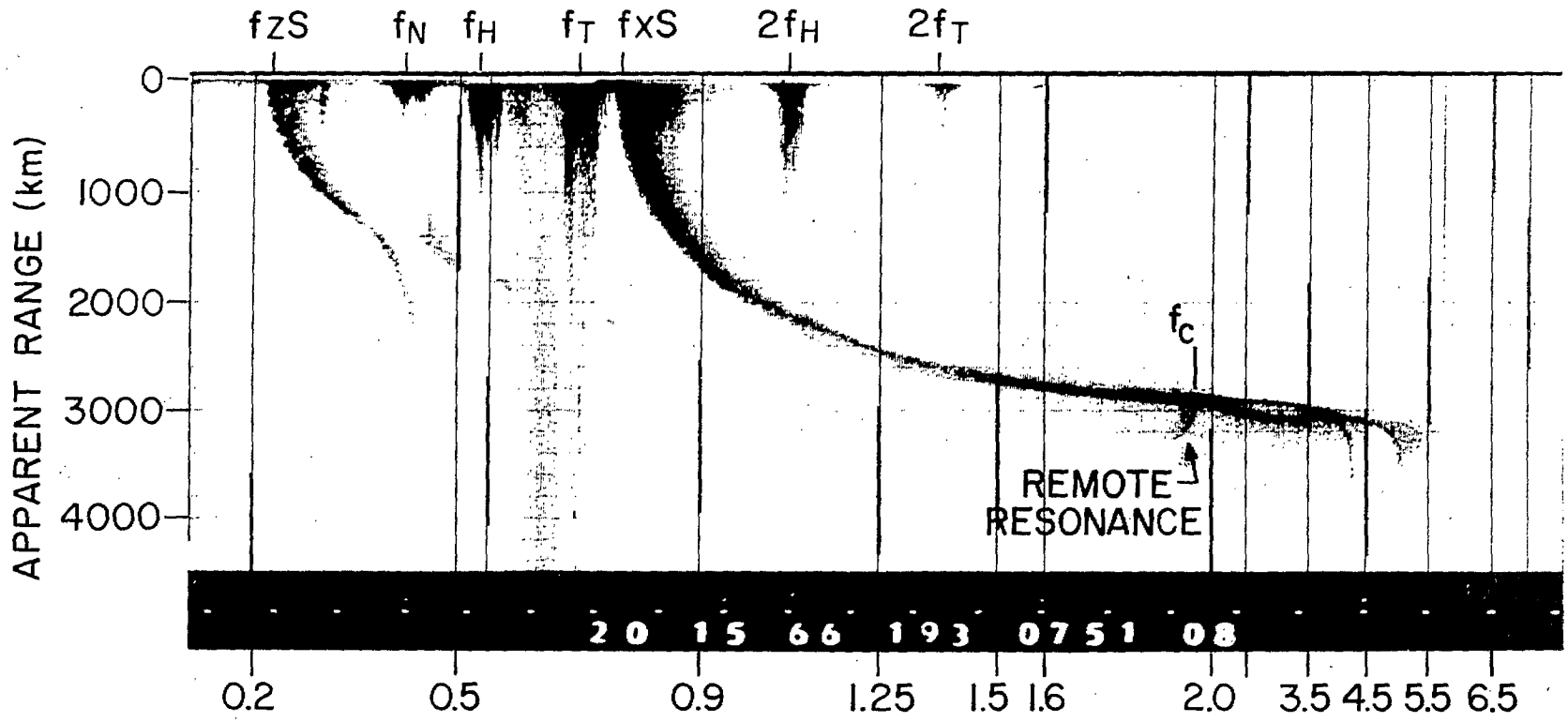

12 JULY 1966 0751/08 GMT (79.5° N, 56.7° E)
SATELLITE HEIGHT 2995 km

FIG 3

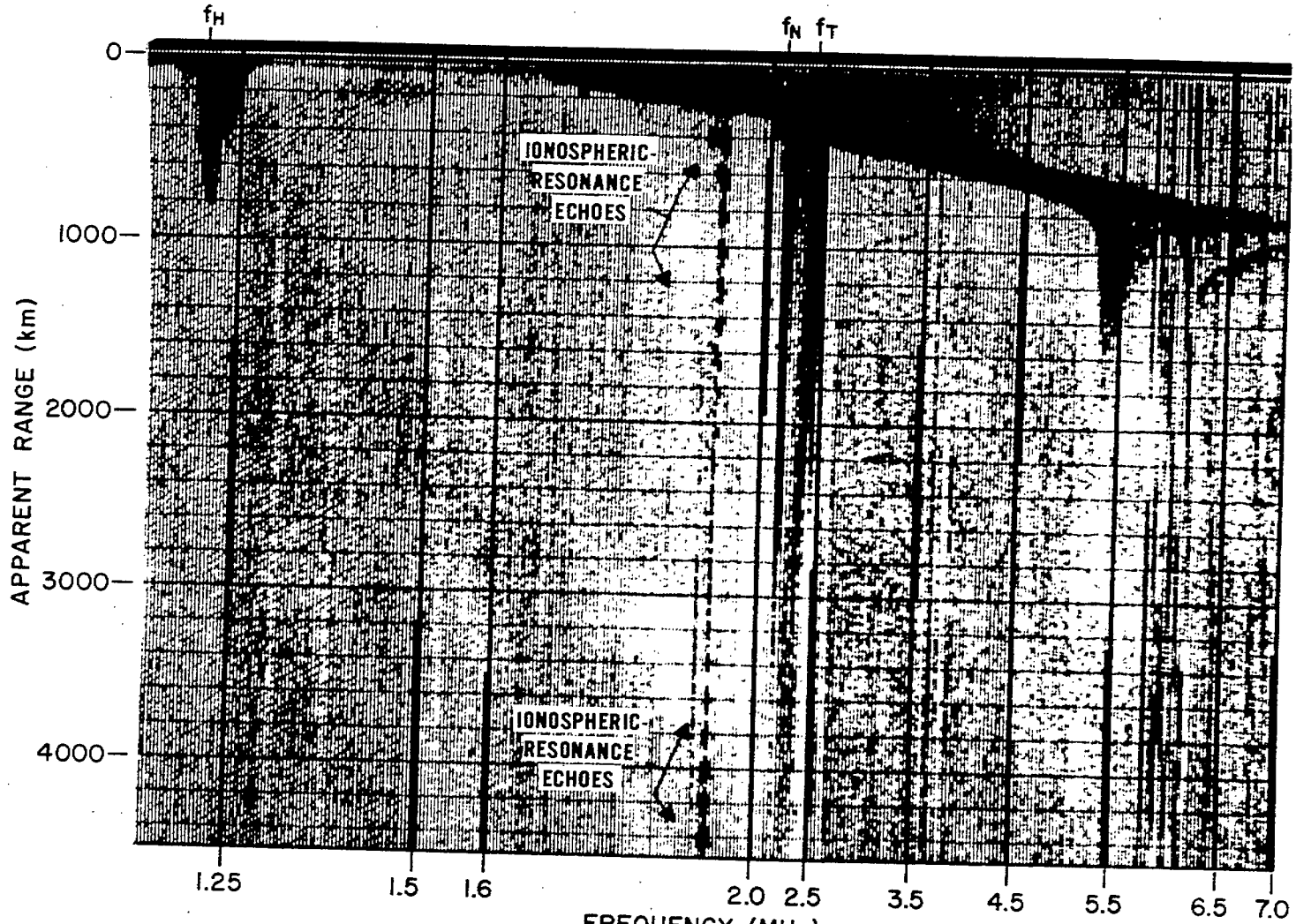

29 APRIL, 1966. 0013/58 GMT (87° W, 76° N)
SATELLITE HEIGHT 677 km

FIG 4

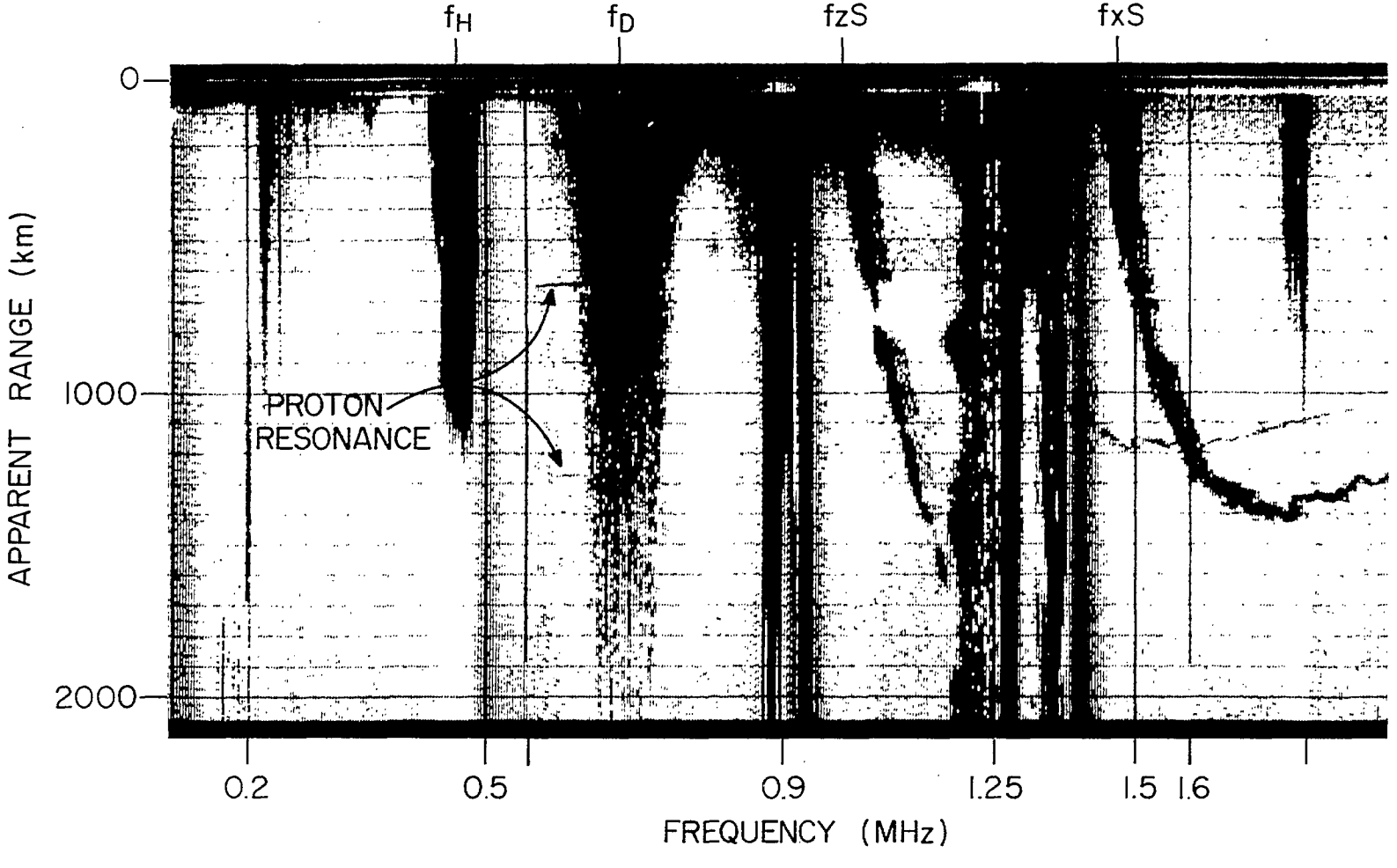

30 DECEMBER 1965 2217/24 GMT (68.2°W, 17.9S)
SATELLITE HEIGHT 1224 km

Fig 5

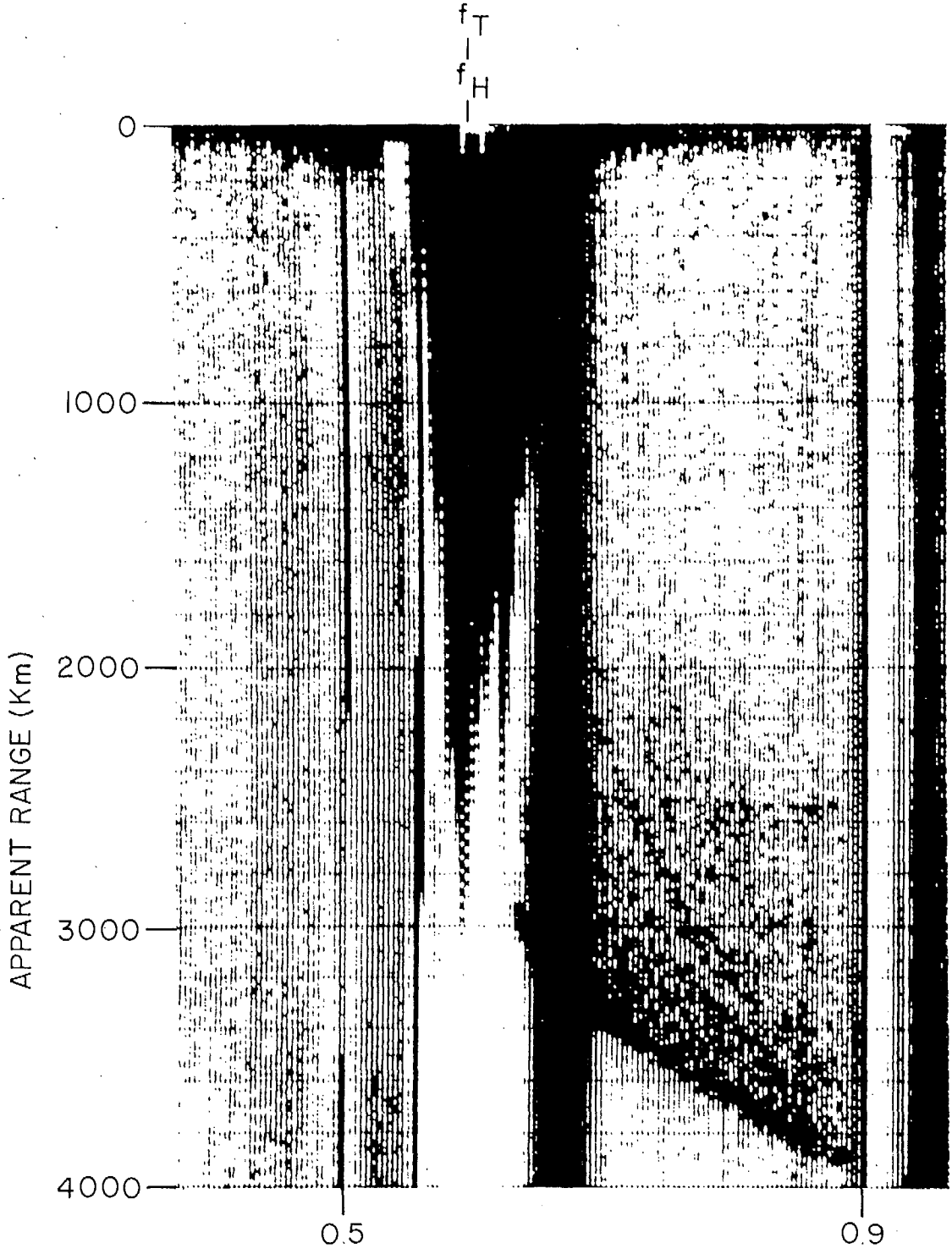
f_T
f_H
0
1000
2000
3000
4000
APPARENT RANGE (Km)
0.5
0.9
FREQUENCY (MHz)
19 DEC. 1965 1409/46 GMT (76°N, 66°W)
SATELLITE HEIGHT 2760 Km

Fig. 6

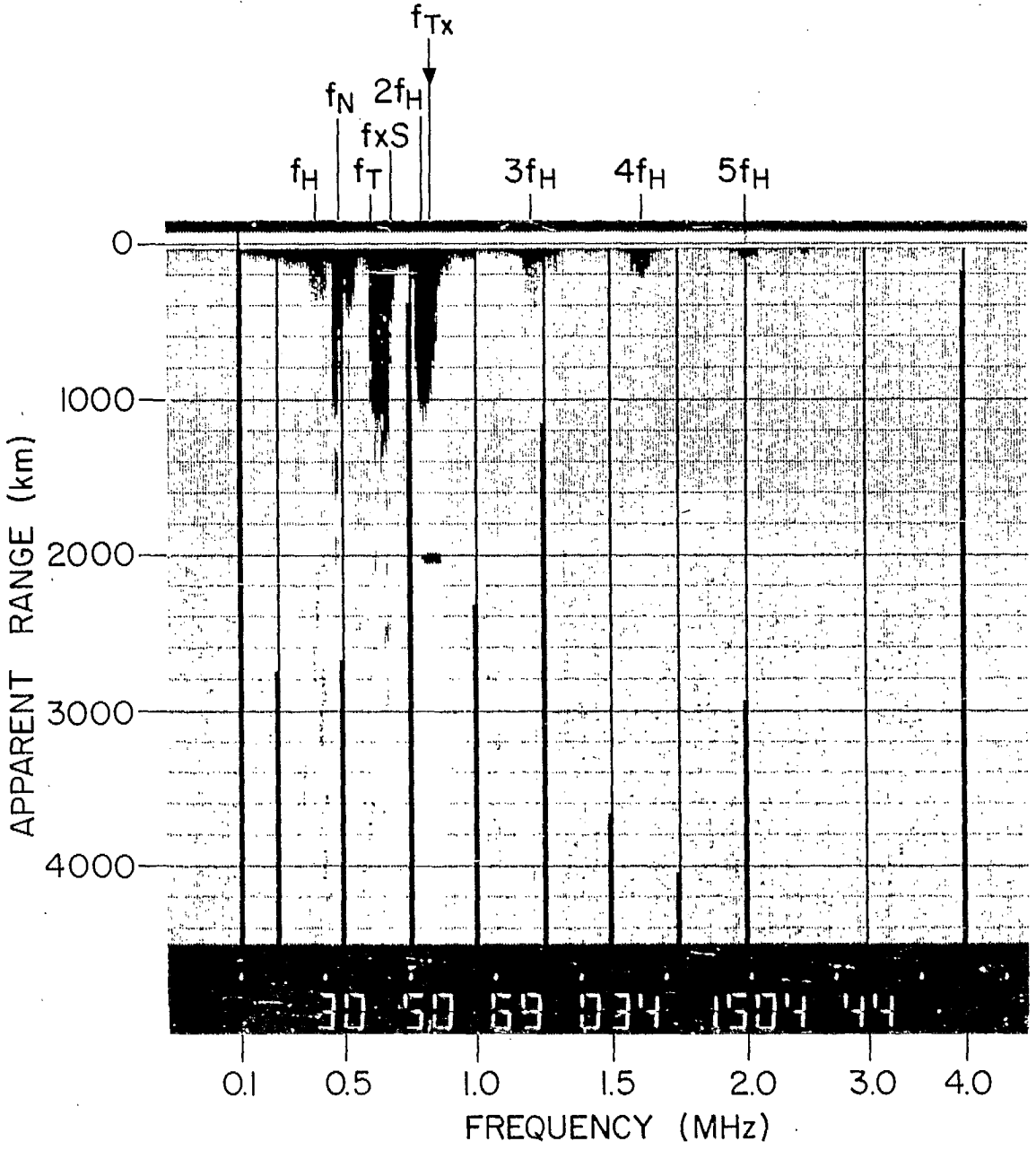

3 FEB. 1969 1504/44 GMT (26°E, 68°S)
SATELLITE HEIGHT 2950 km

Fig 6a

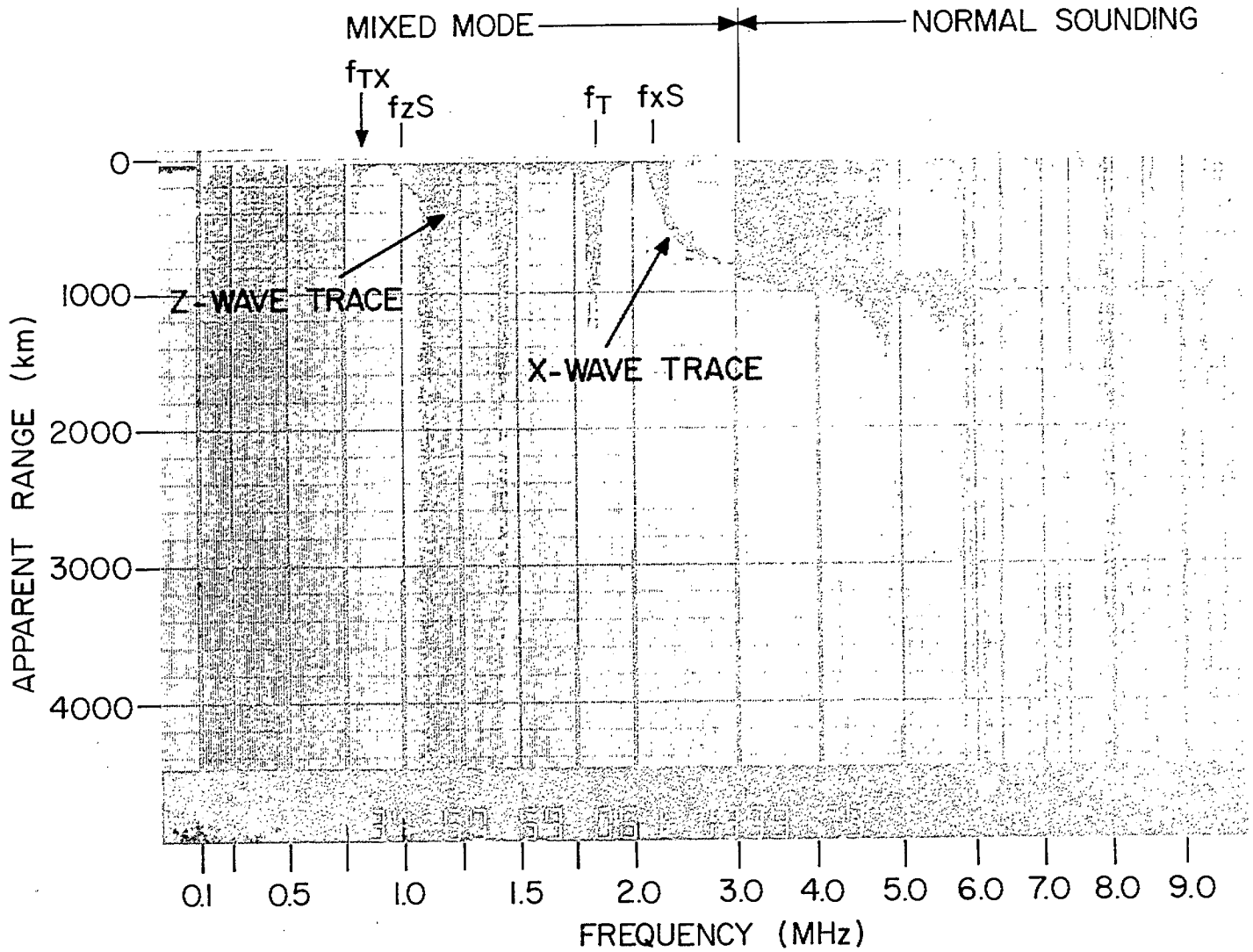

2 MARCH 1969 1339/19 GMT (59°N, 74°W)
SATELLITE HEIGHT 963 km

Fig 6b

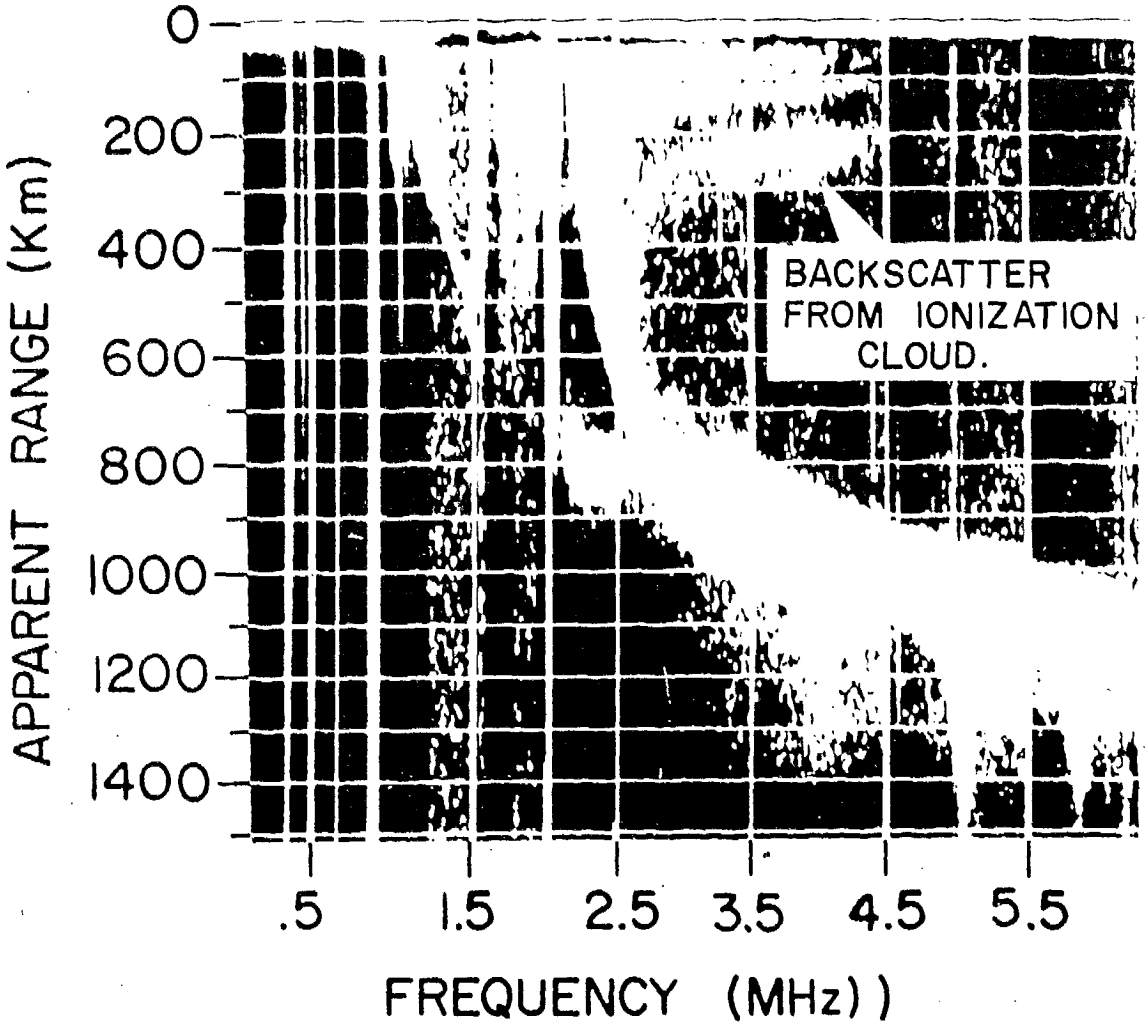

1 OCT. 1962, 15:43 GMT (63°W, 64°N)
SATELLITE HEIGHT 1029 Km

FIG 7

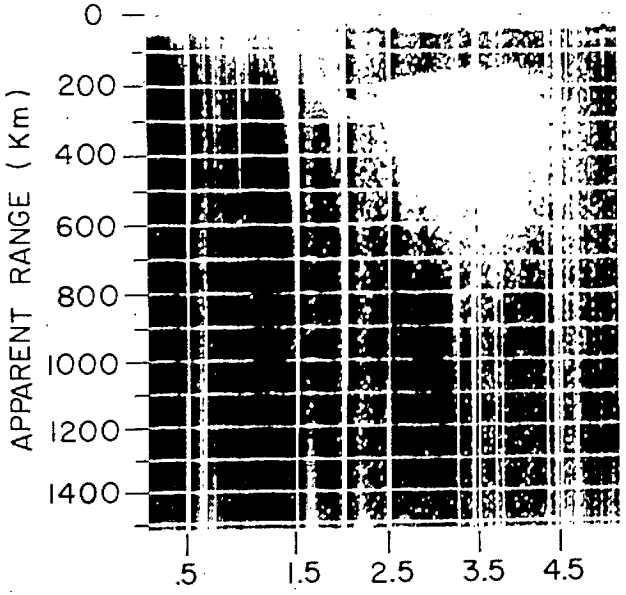

18 OCT. 1962 00:35 GMT (63.9°W, 20.7°N)
SATELLITE HEIGHT 1019 Km

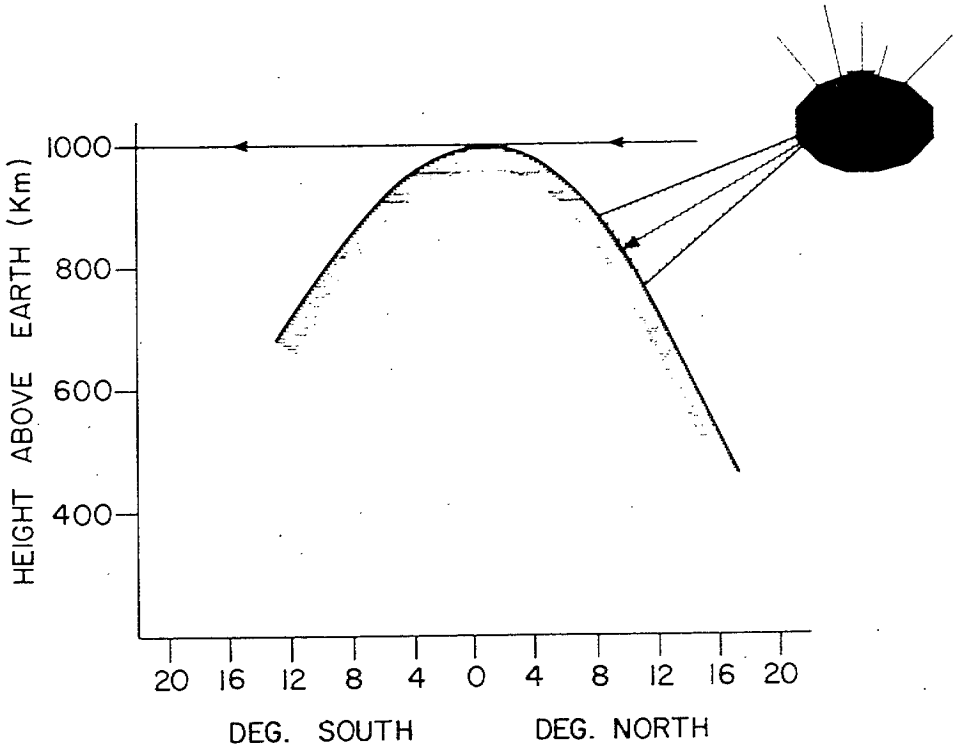

Fig 8

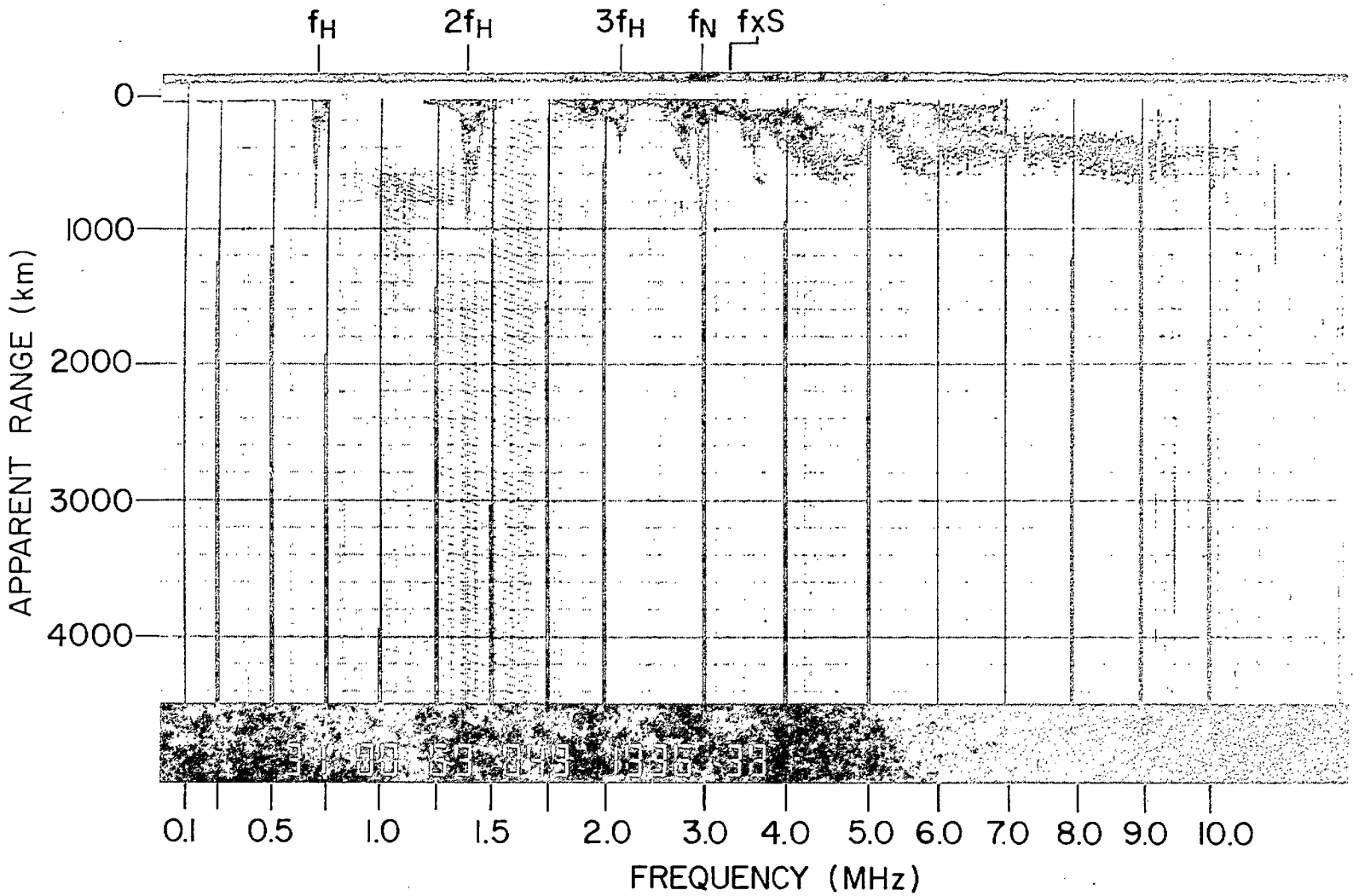

18 FEB. 1968 1936/38 GMT (26°N, 17°E)
SATELLITE HEIGHT 733 km

Fig 9a

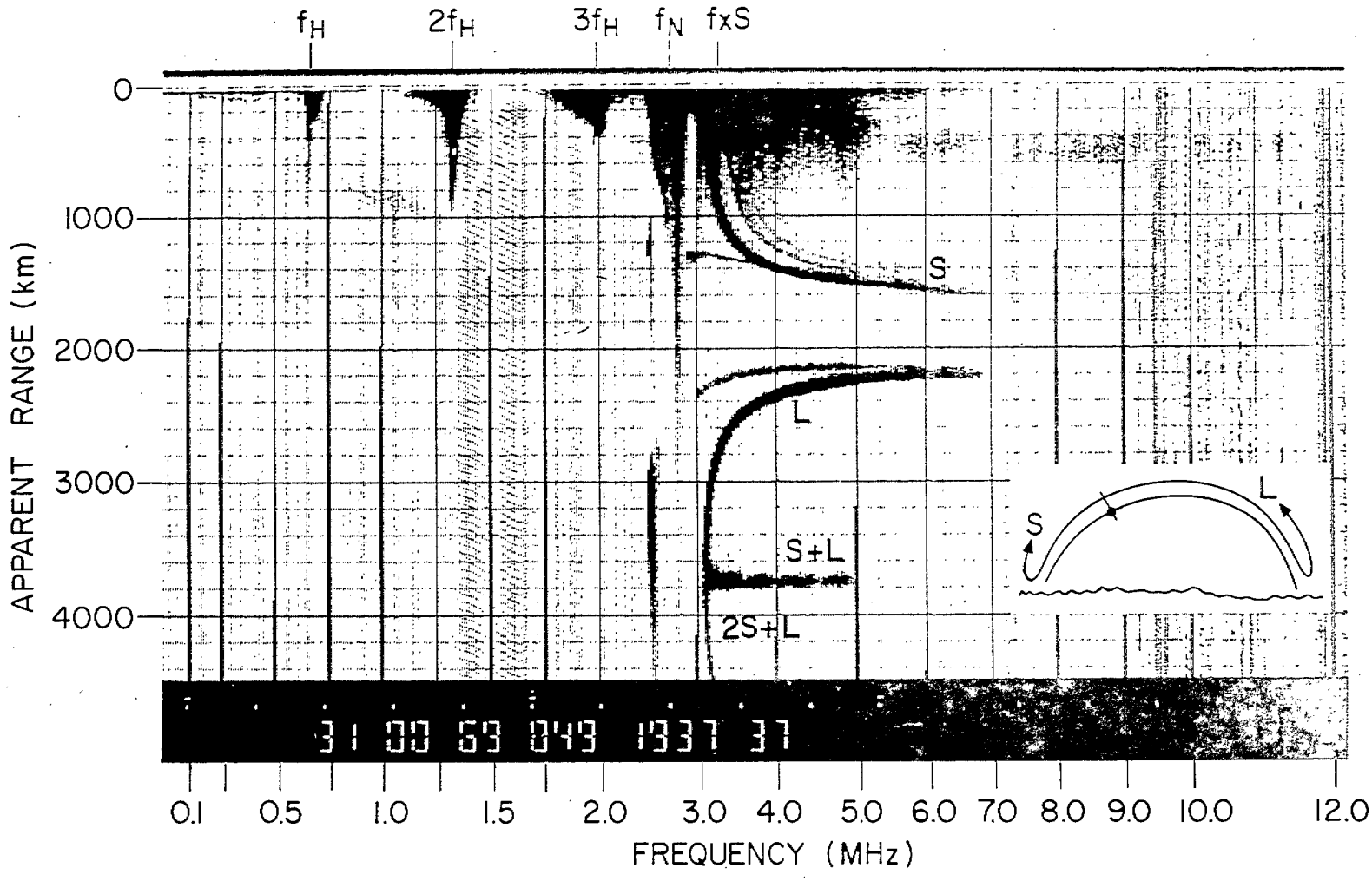

18 FEB. 1968 1937/37 GMT (26°N, 13°E)
SATELLITE HEIGHT 771 km

FIG 9b

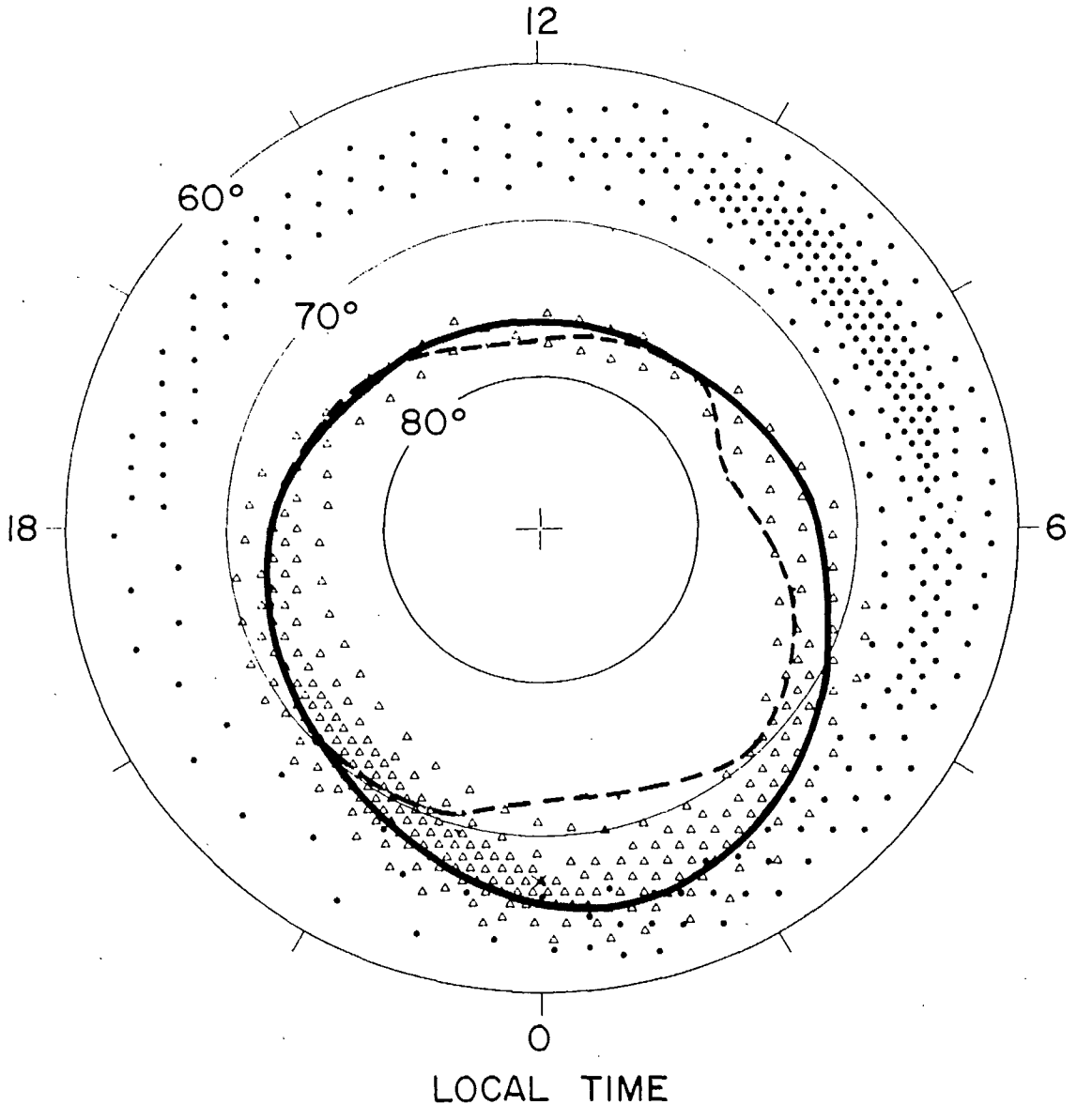

Fig 10

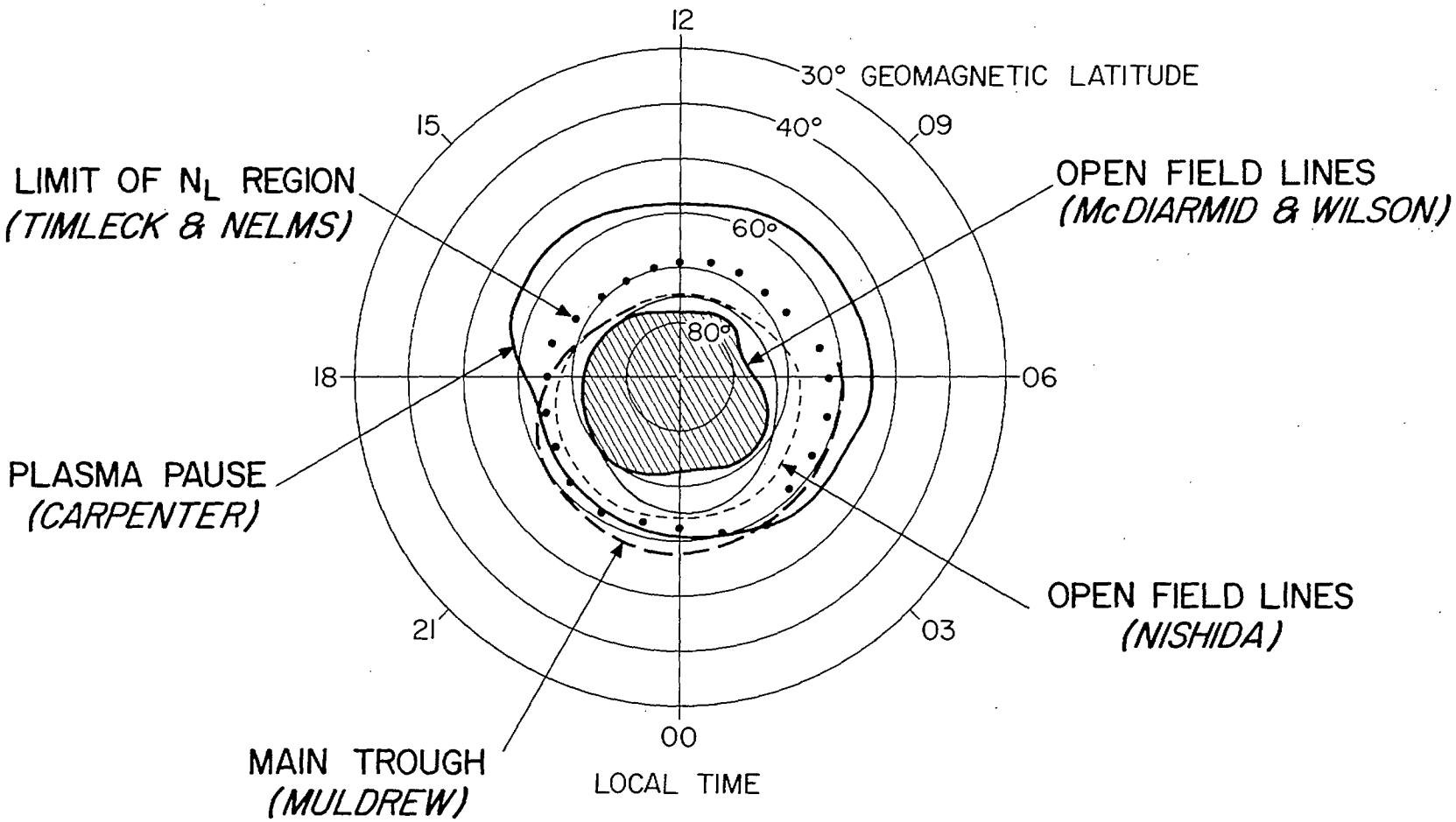
12
30° GEOMAGNETIC LATITUDE
40°
09
15
LIMIT OF N_L REGION
(TIMLECK & NELMS)
60°
OPEN FIELD LINES
(McDIARMID & WILSON)
80°
18
06
PLASMA PAUSE
(CARPENTER)
OPEN FIELD LINES
(NISHIDA)
21
03
00
MAIN TROUGH
(MULDREW)
LOCAL TIME

FIG 11

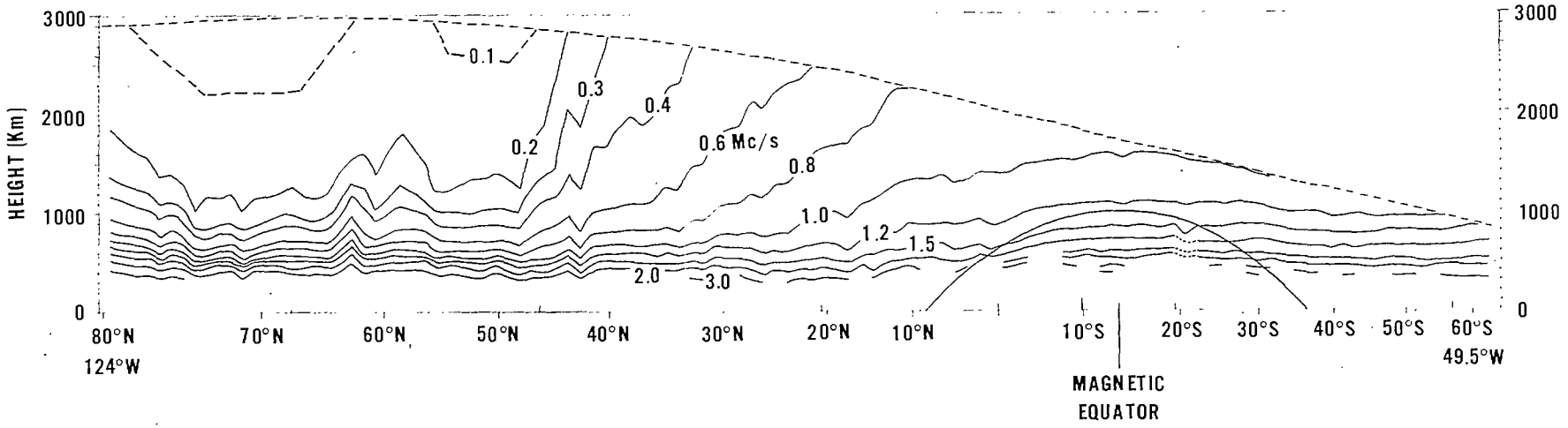

19 DECEMBER 1965 (2259 HRS. GMT.) Kp=4-

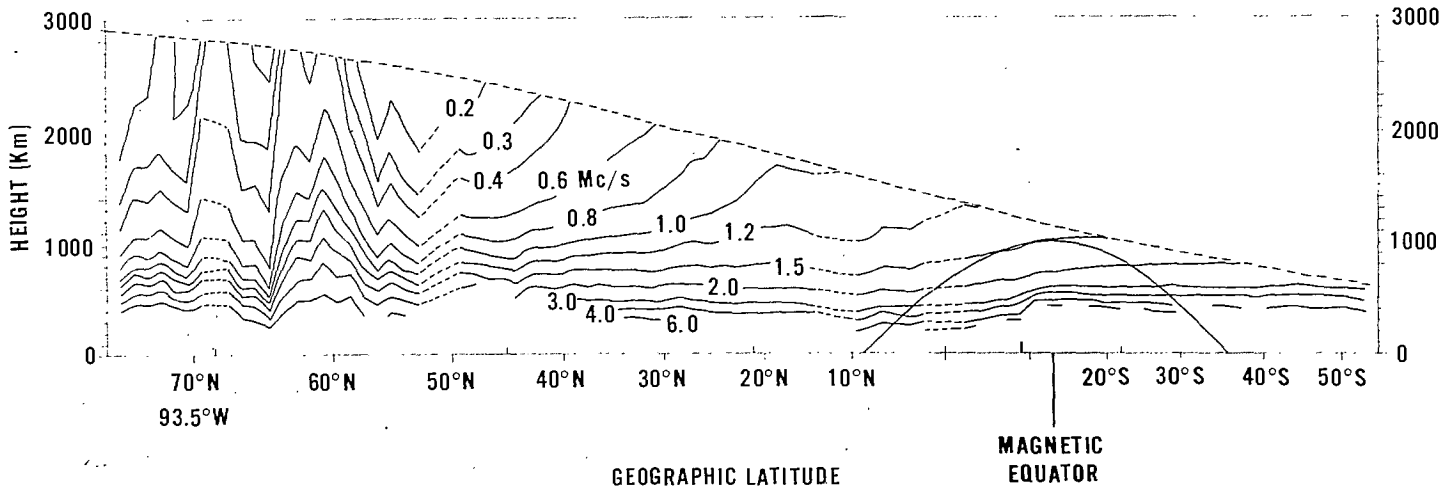

4 JANUARY 1966 (2138 HRS. GMT.) Kp=3

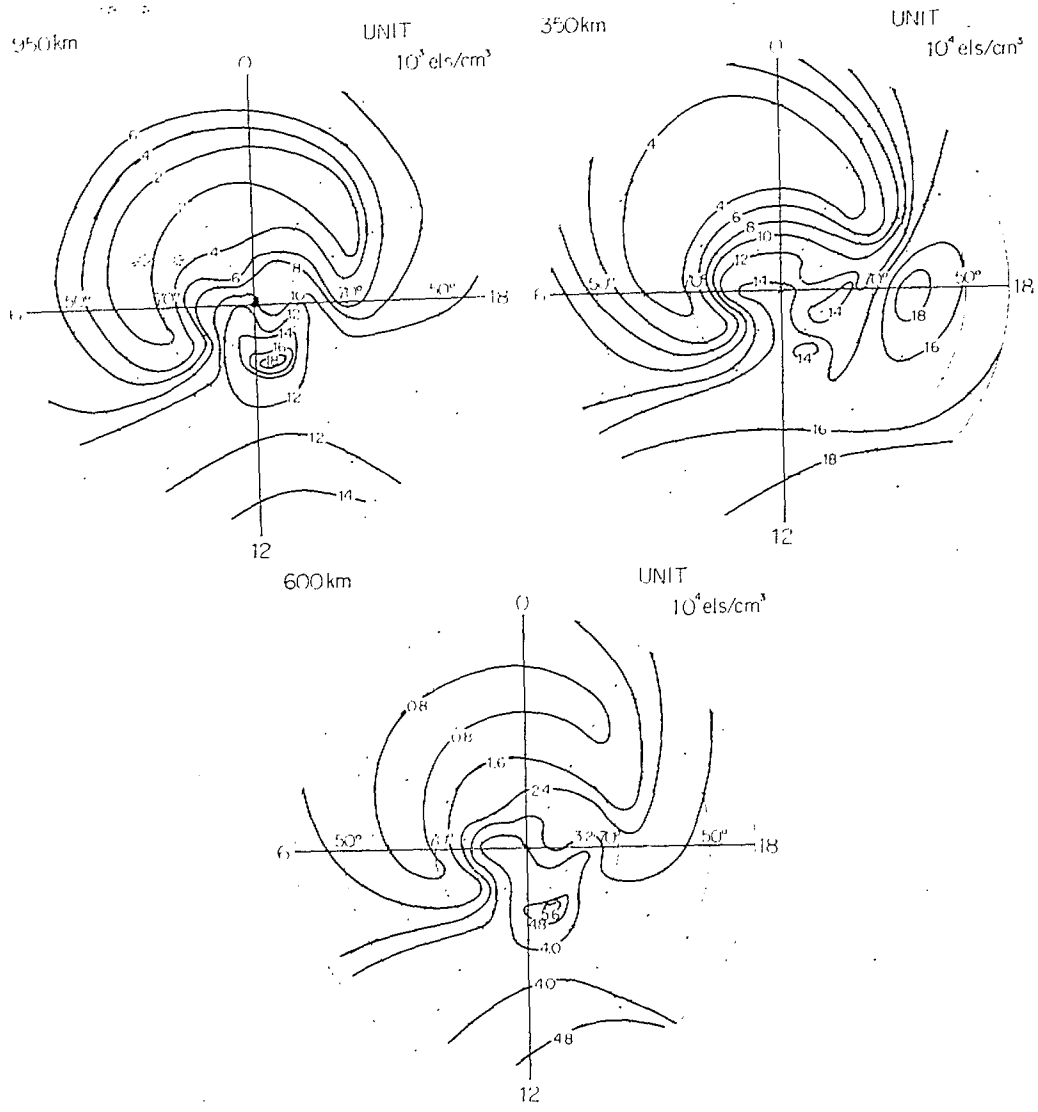
950km
UNIT
10³ els/cm³
0
6
12
18
12
350km
UNIT
10⁴ els/cm³
0
6
12
18
12
600km
UNIT
10⁴ els/cm³
0
6
12
18
12

FIG 13

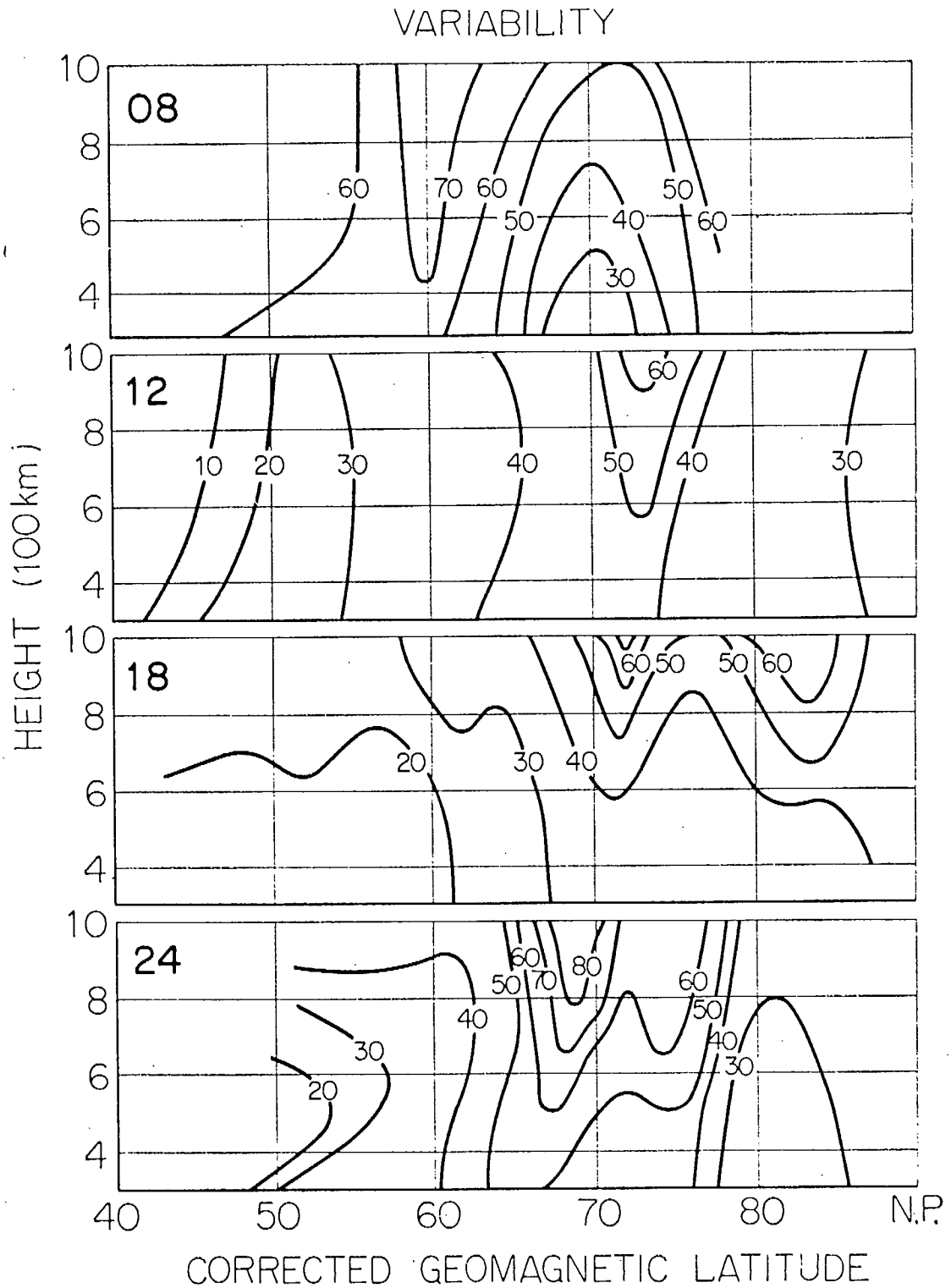
VARIABILITY
08
12
18
24
HEIGHT (100km)
10
8
6
4
60
70
50
40
30
20
10
40
50
60
70
80
N.P.
CORRECTED GEOMAGNETIC LATITUDE

FIG 14

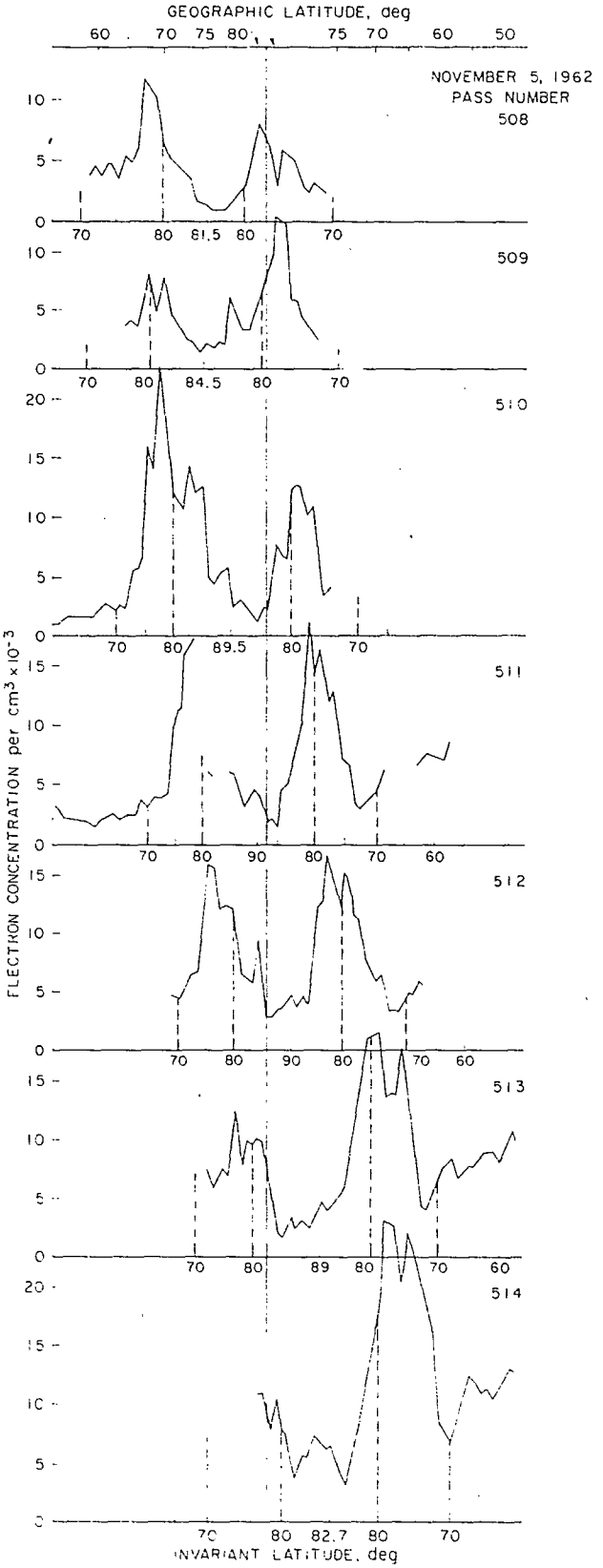
GEOGRAPHIC LATITUDE, deg
60 70 75 80 75 70 60 50
NOVEMBER 5, 1962
PASS NUMBER
508
509
510
511
512
513
514
FLECTRON CONCENTRATION per cm^3 x10^{-3}
70 80 81.5 80 70
70 80 84.5 80 70
70 80 89.5 80 70
70 80 90 80 70 60
70 80 90 80 70 60
70 80 89 80 70 60
70 80 82.7 80 70
INVARIANT LATITUDE, deg

FIG 15

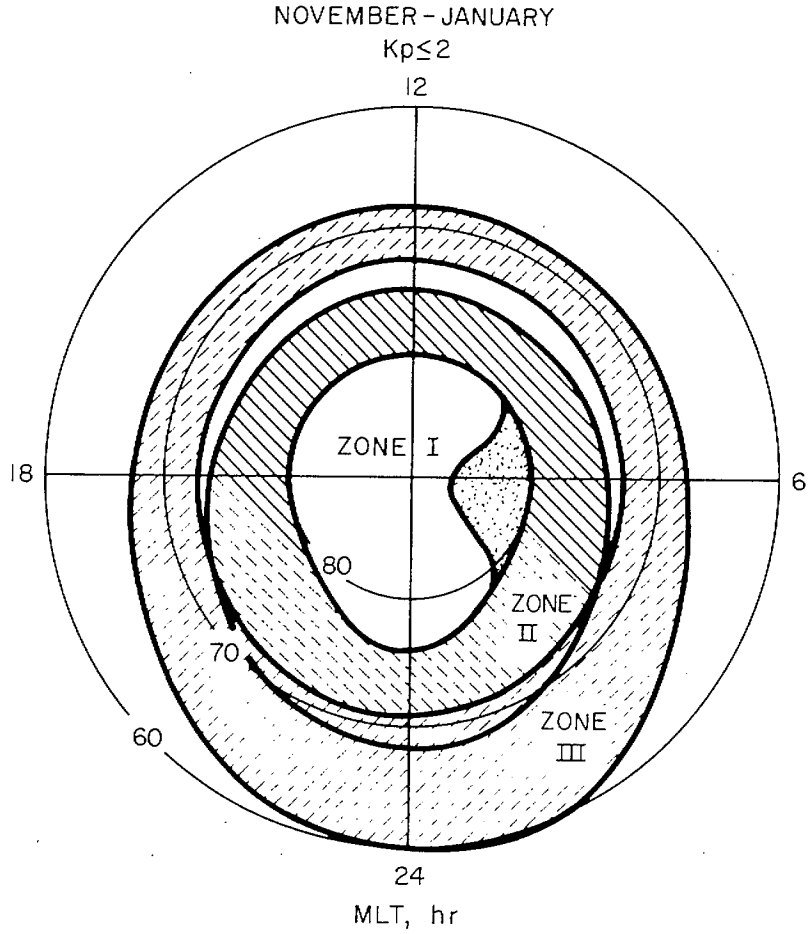
NOVEMBER - JANUARY
Kp≤2
12
18
6
24
60
70
80
ZONE I
ZONE II
ZONE III
MLT, hr

(a)

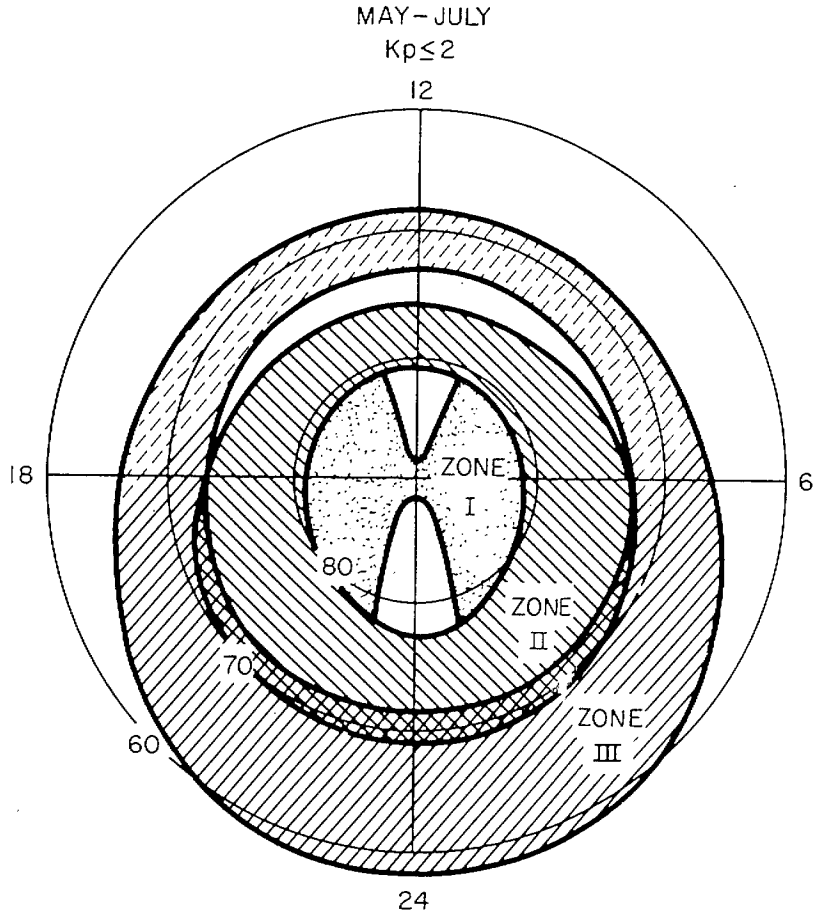
MAY - JULY
Kp≤2
12
18
6
24
60
70
80
ZONE I
ZONE II
ZONE III

(b)

FIG 16

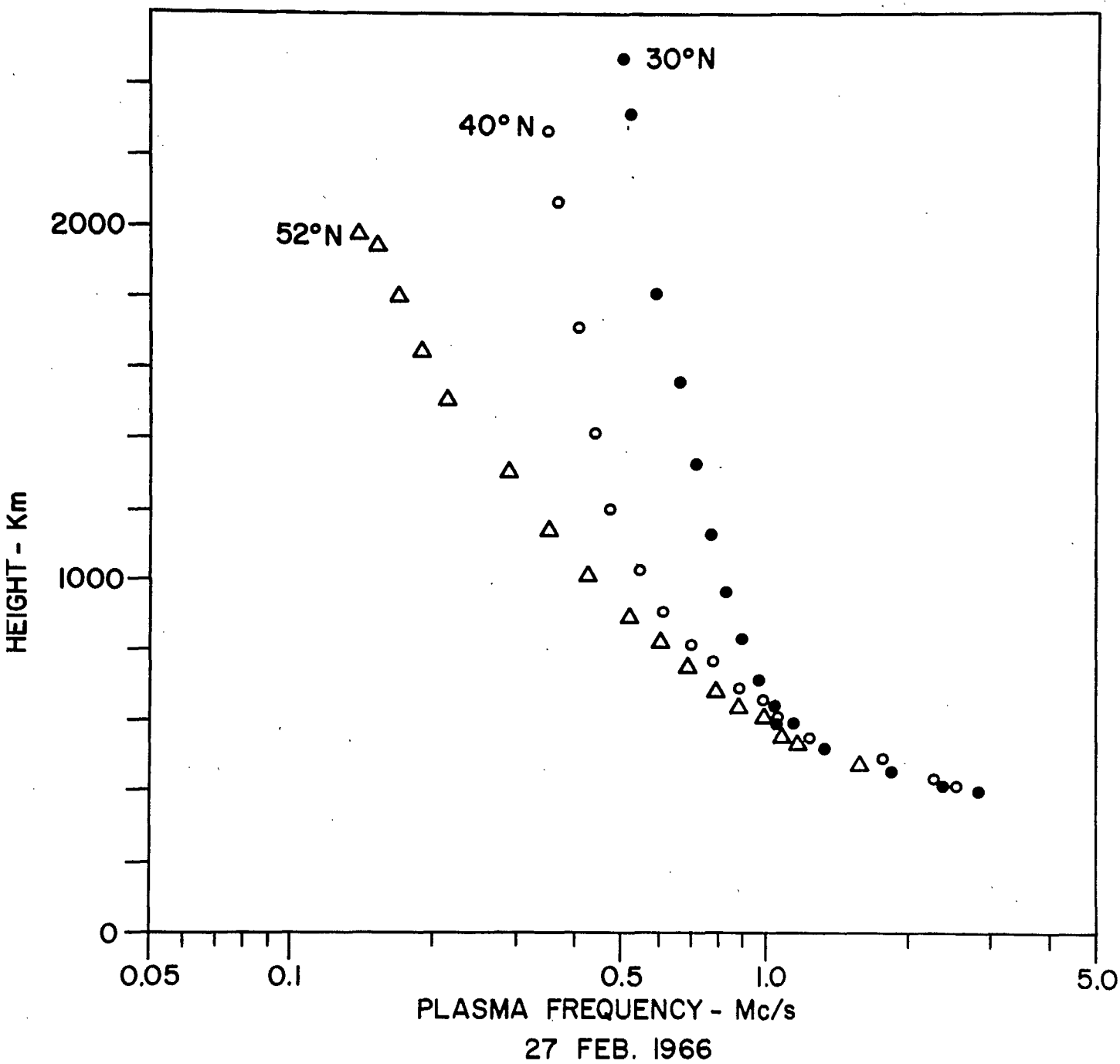
30°N
40°N
52°N
2000
1000
0
HEIGHT - Km
0.05
0.1
0.5
1.0
5.0
PLASMA FREQUENCY - Mc/s
27 FEB. 1966

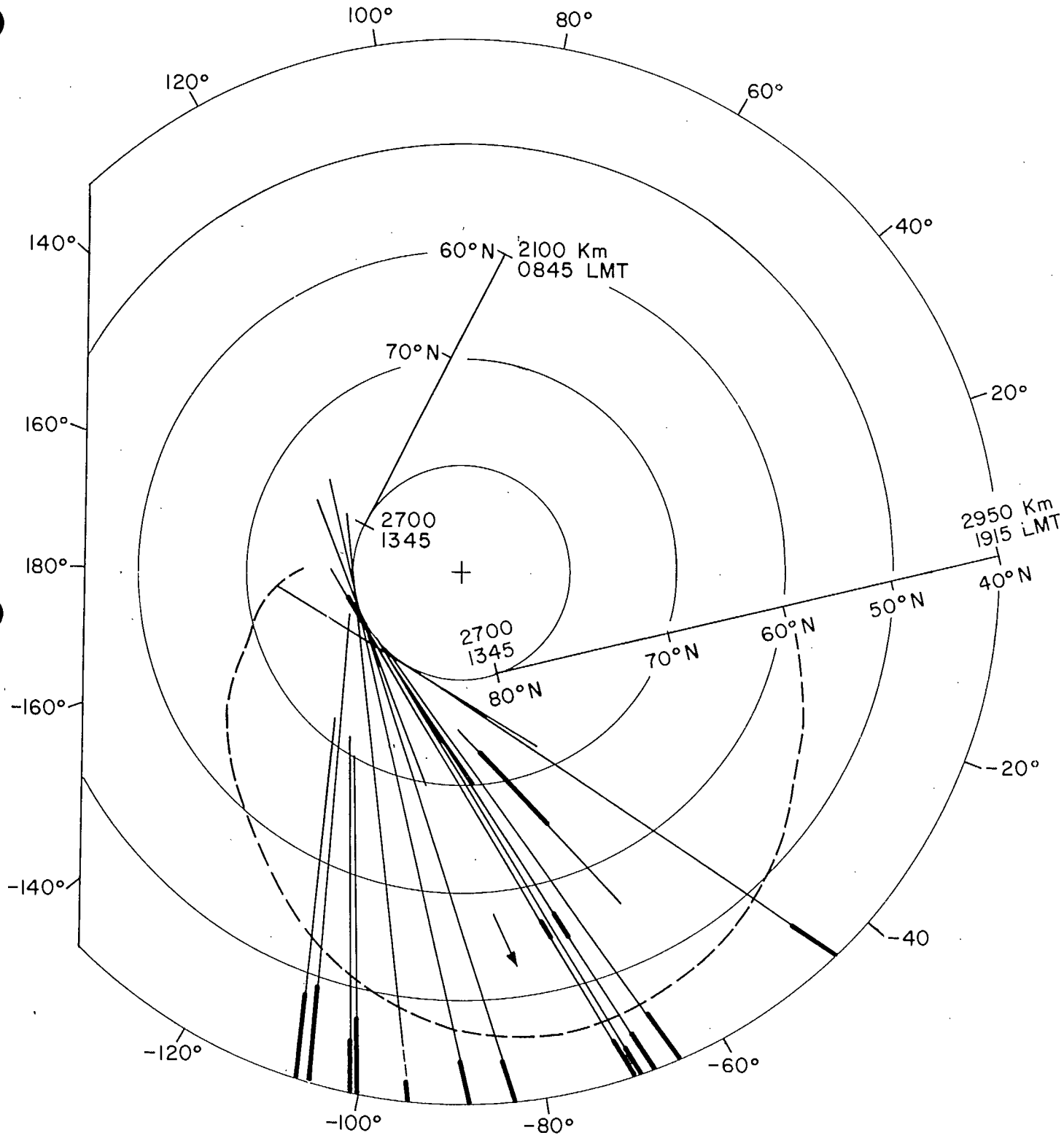

1 TO 15 DECEMBER 1965

FIG 13

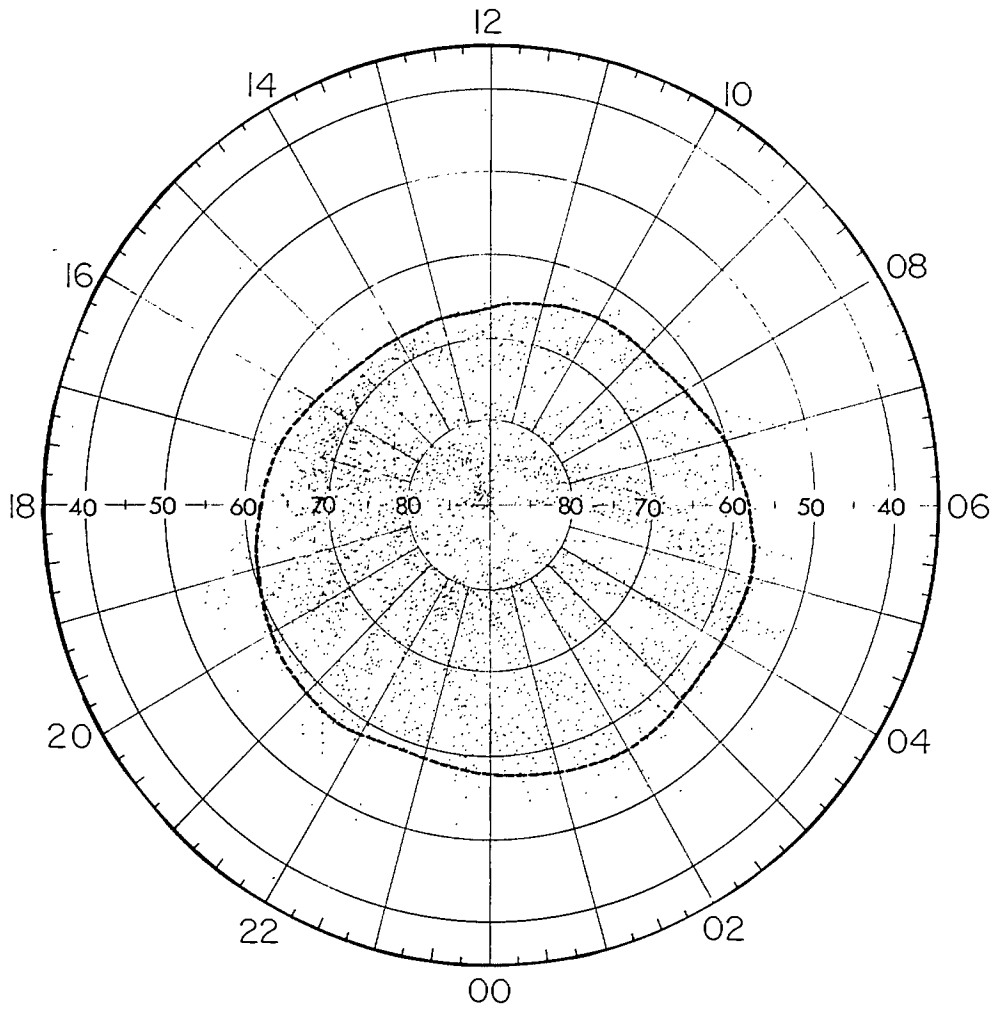

LOCAL TIME VS GEOMAGNETIC LATITUDE

FIG 19

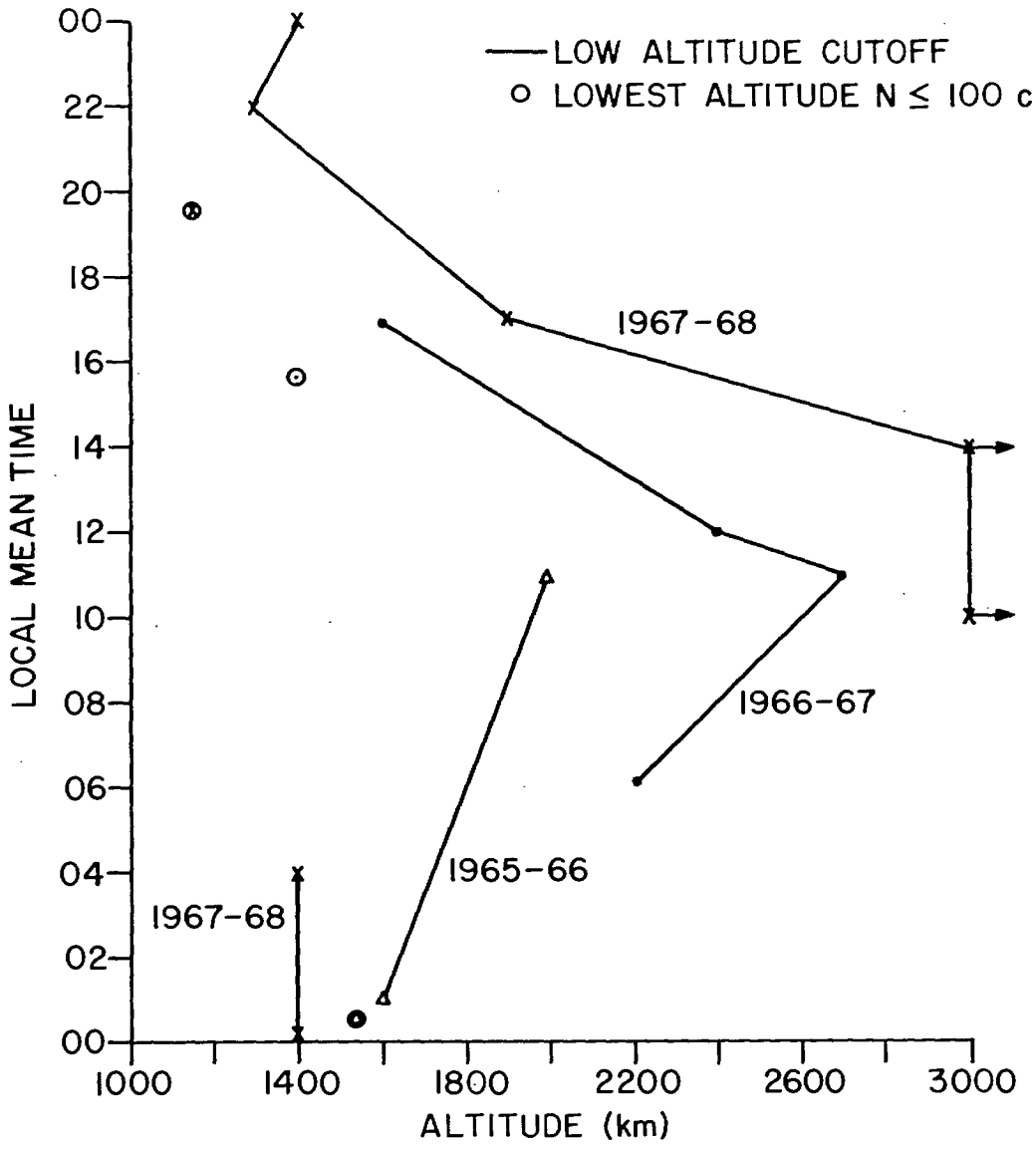
LOW ALTITUDE CUTOFF
LOWEST ALTITUDE N ≤ 100 cm⁻³
1967-68
1966-67
1965-66
1967-68
LOCAL MEAN TIME
00
22
20
18
16
14
12
10
08
06
04
02
00
1000
1400
1800
2200
2600
3000
ALTITUDE (km)

Fig 20

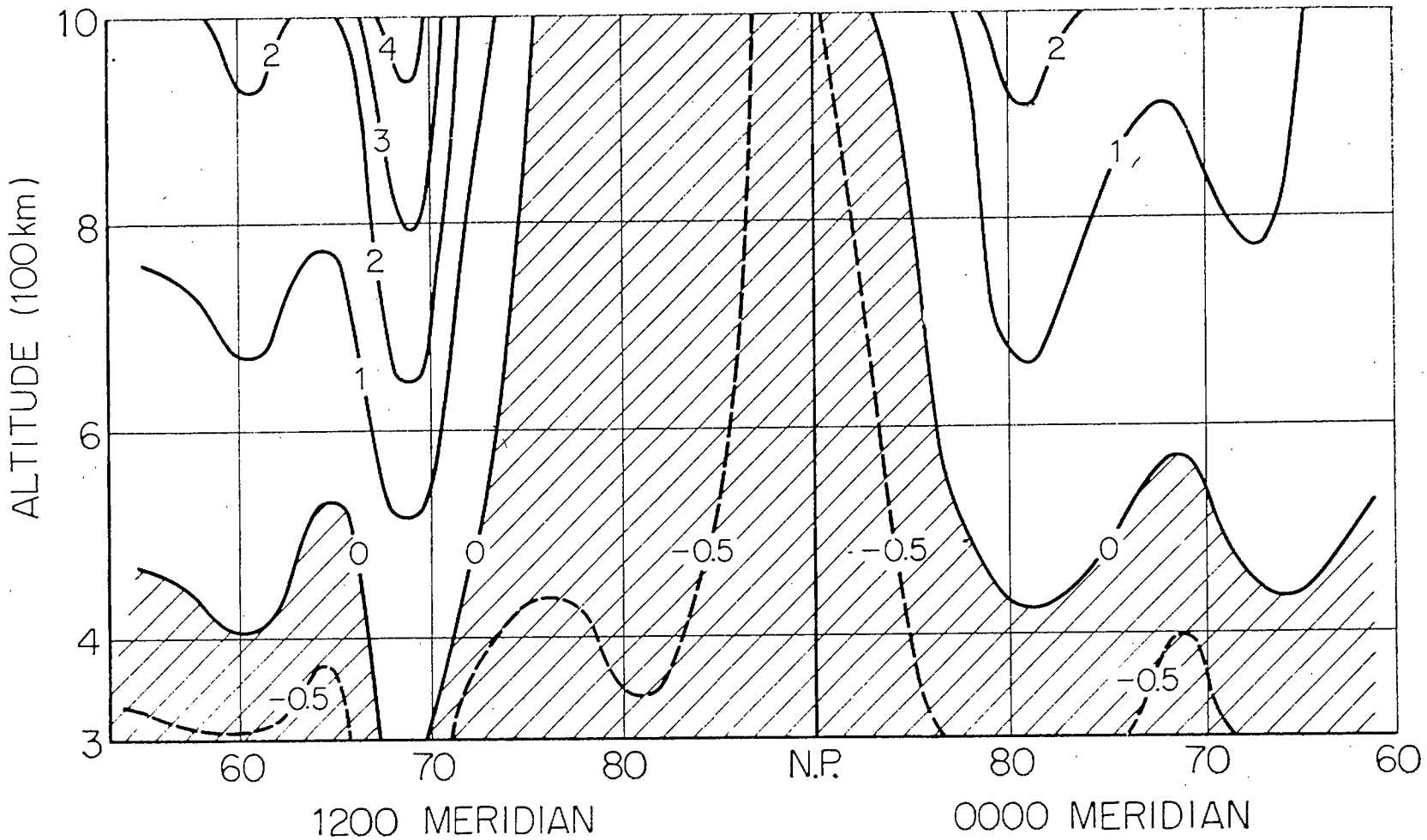
ALTITUDE (100km)
10
8
6
4
3
60
70
80
N.P.
80
70
60
1200 MERIDIAN
0000 MERIDIAN
2
4
3
2
1
0
0
−0.5
−0.5
−0.5
2
1
0
−0.5

FIG 21

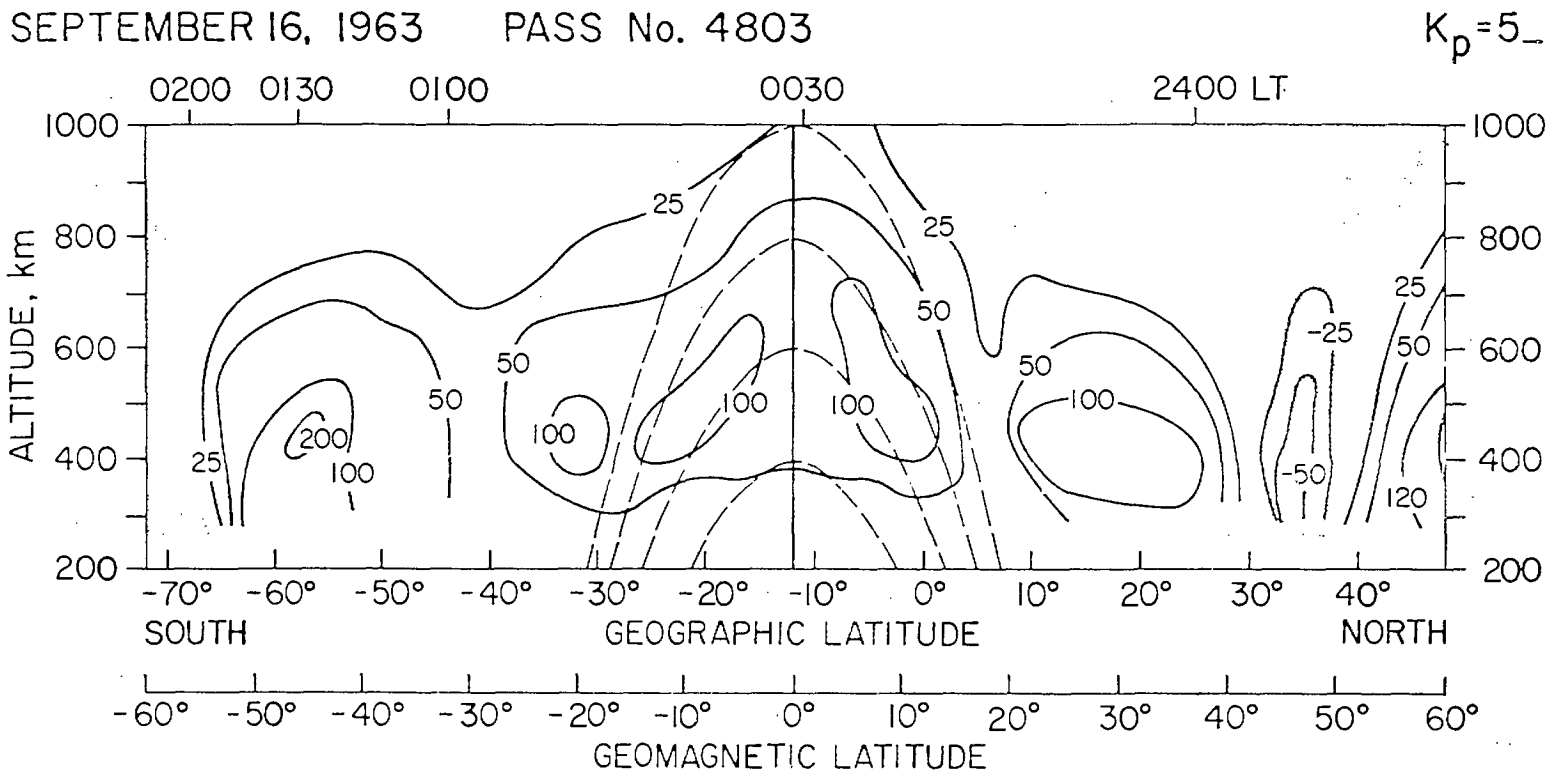
SEPTEMBER 16, 1963 PASS No. 4803
K_p=5-
0200 0130 0100 0030 2400 LT
ALTITUDE, km
1000
800
600
400
200
25
50
100
200
-25
-50
120
-70° -60° -50° -40° -30° -20° -10° 0° 10° 20° 30° 40°
SOUTH
GEOGRAPHIC LATITUDE
NORTH
-60° -50° -40° -30° -20° -10° 0° 10° 20° 30° 40° 50° 60°
GEOMAGNETIC LATITUDE

FIG 22

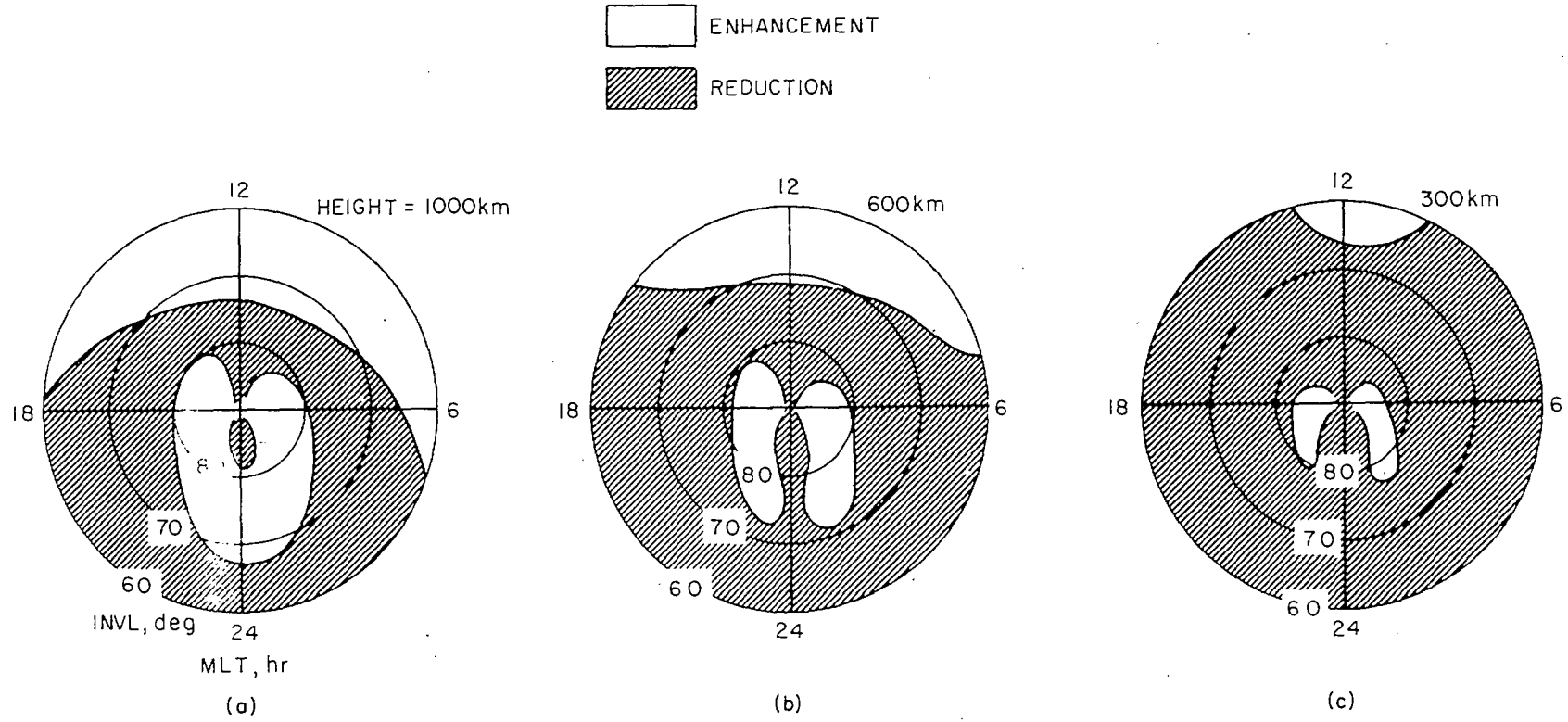
ENHANCEMENT
REDUCTION
12
HEIGHT = 1000km
18
6
70
60
INVL, deg
24
MLT, hr
(a)
12
600km
18
6
80
70
60
24
(b)
12
300km
18
6
80
70
60
24
(c)

Fig 23

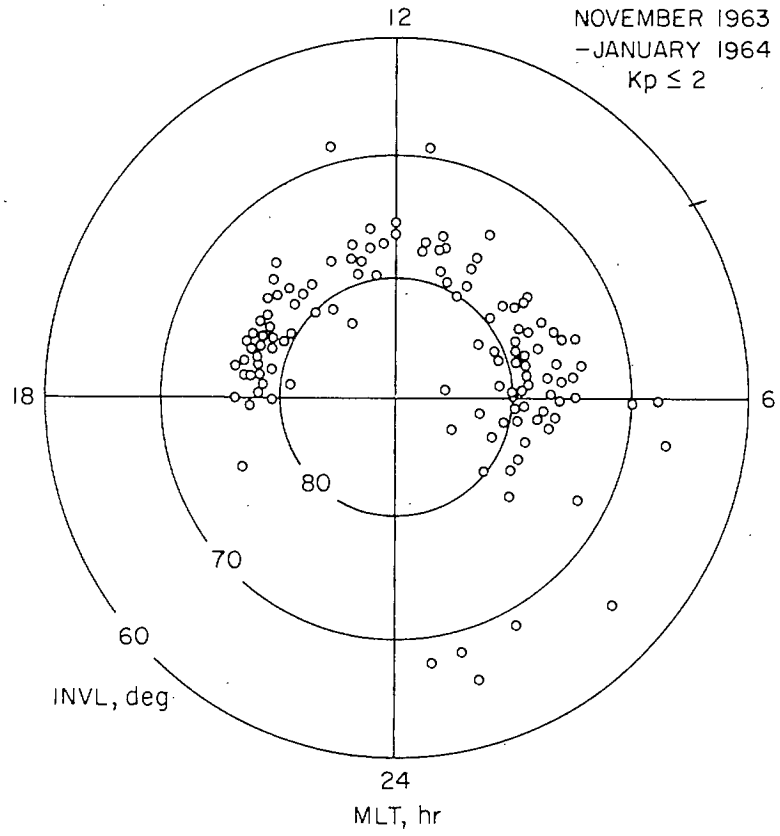
12
NOVEMBER 1963
–JANUARY 1964
Kp ≤ 2
18
6
80
70
60
INVL, deg
24
MLT, hr

(a)

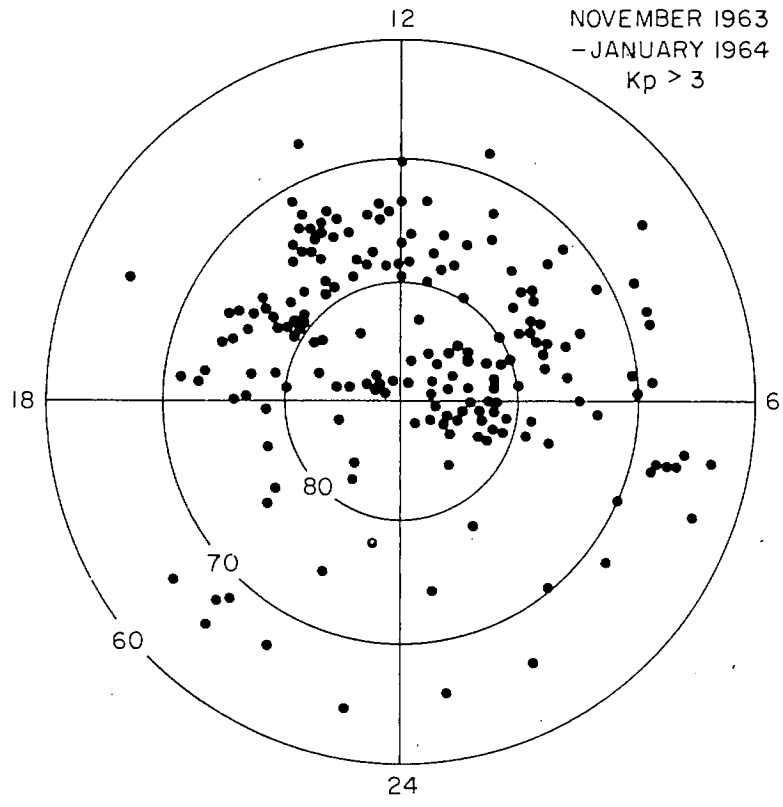
12
NOVEMBER 1963
–JANUARY 1964
Kp > 3
18
6
80
70
60
24

(b)

Fig 24

TOPSIDE SOUNDING DATA FROM ALOUETTE 1
(0036 to 0052 GMT) 23 SEPTEMBER 1963 Kp 9

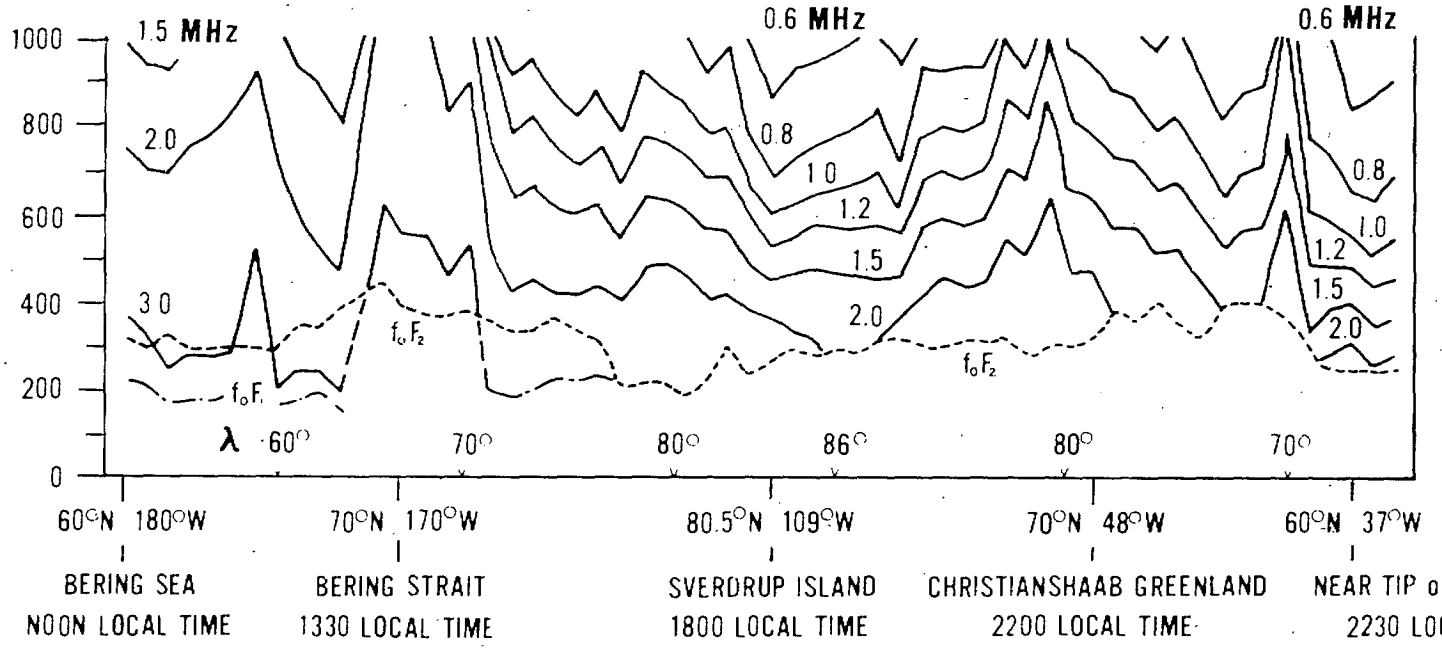

CONTOURS OF CONSTANT PLASMA FREQUENCY ELECTRON DENSITY
ACROSS THE ARCTIC FROM SIBERIA TO GREENLAND DURING THE SEPTEMBER 1963 MAGNETIC STORM

FIG. 25

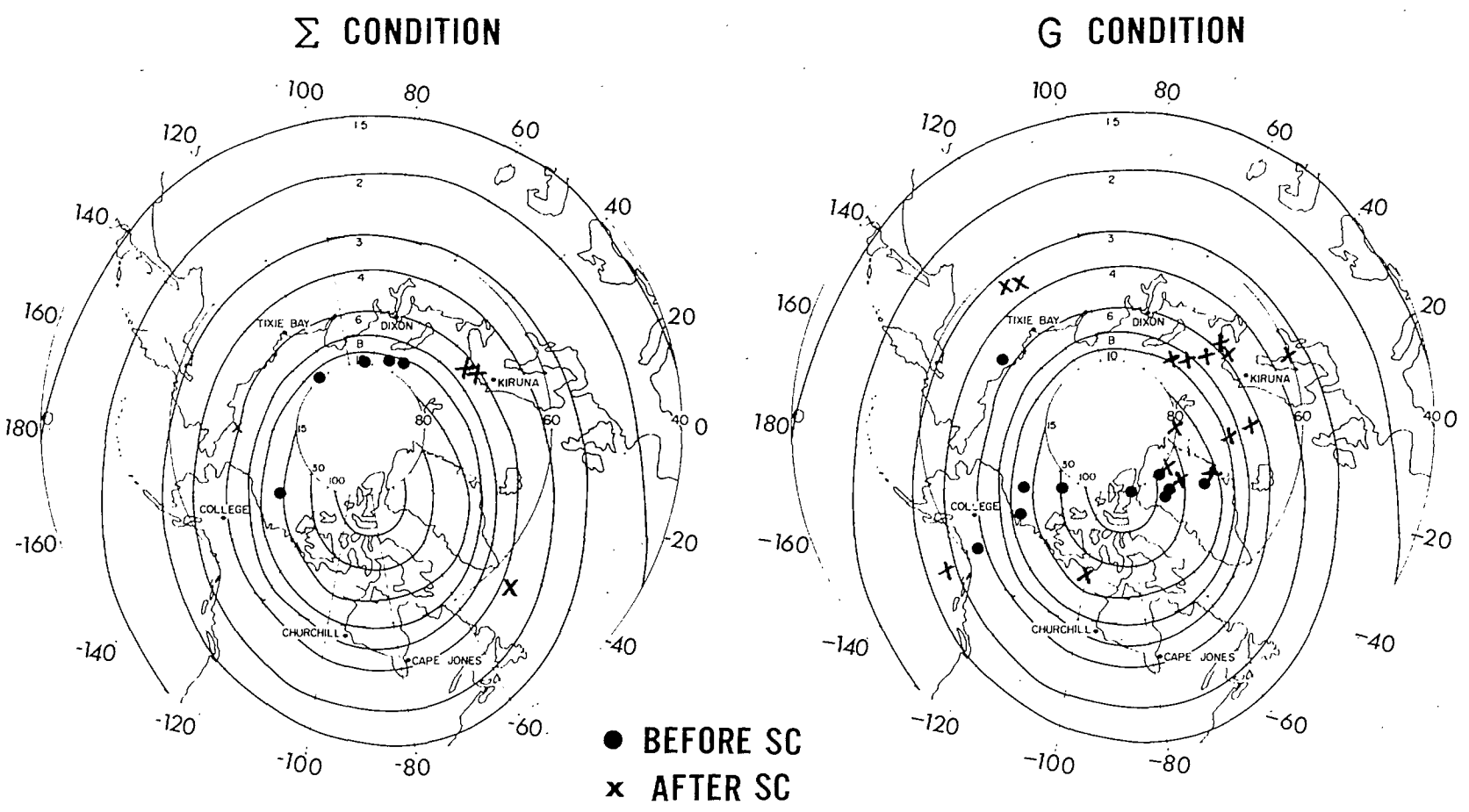
Σ CONDITION
G CONDITION
TIXIE BAY
DIXON
KIRUNA
COLLEGE
CHURCHILL
CAPE JONES
● BEFORE SC
x AFTER SC

FIG 26

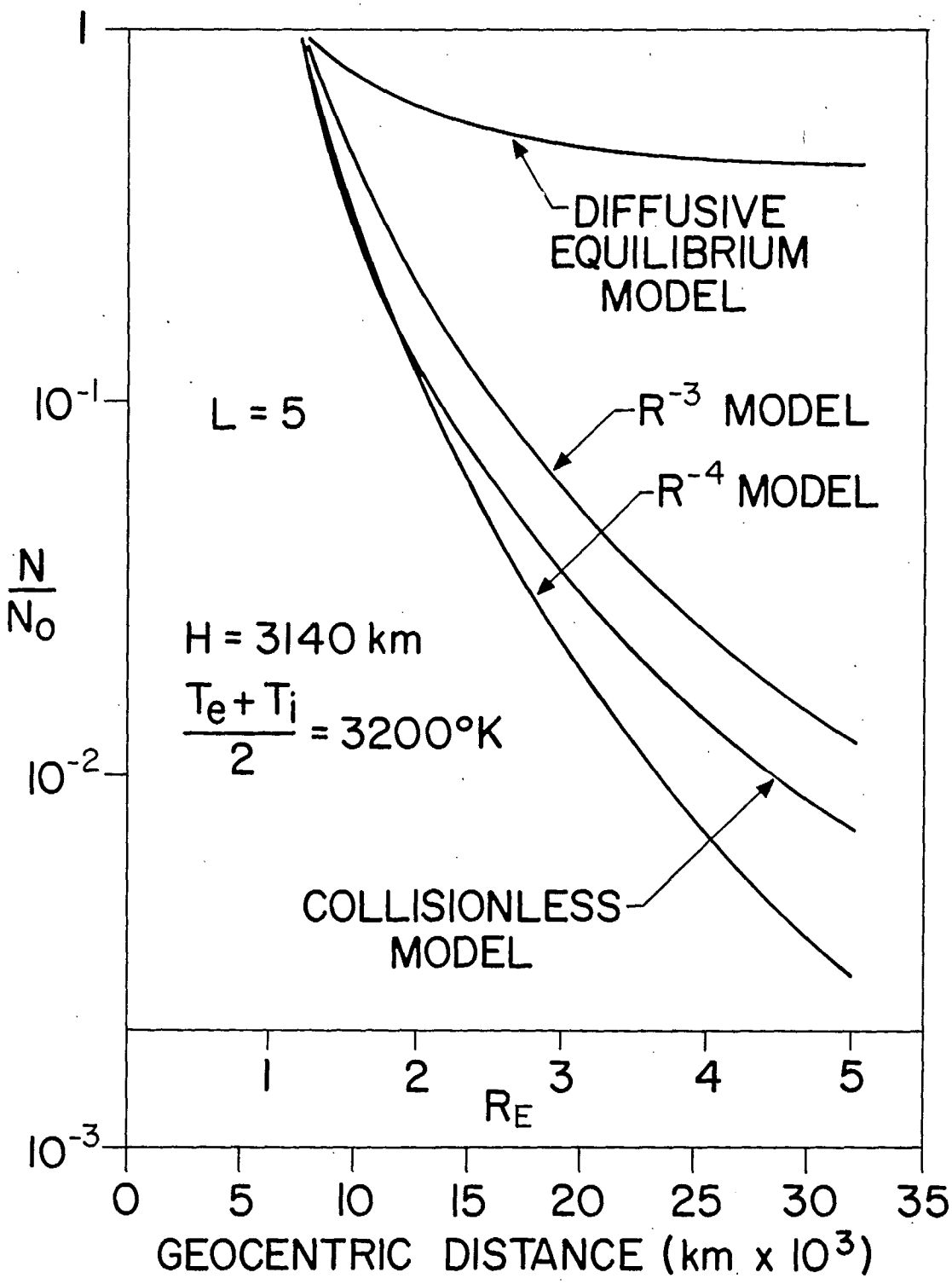
1
10^{-1}
10^{-2}
10^{-3}
$\frac{N}{N_o}$
L = 5
H = 3140 km
$\frac{T_e + T_i}{2}$ = 3200°K
DIFFUSIVE EQUILIBRIUM MODEL
R^{-3} MODEL
R^{-4} MODEL
COLLISIONLESS MODEL
1 2 3 4 5
R_E
0 5 10 15 20 25 30 35
GEOCENTRIC DISTANCE (km x 10^3)

FIG 27